Article:
Obande, W., Ó Brádaigh, C.M. and Ray, D. (2021) Continuous fibre-reinforced thermoplastic acrylic-matrix composites prepared by liquid resin infusion – a review. Composites Part B: Engineering, 215. 108771. ISSN: 1359-8368

https://doi.org/10.1016/j.compositesb.2021.108771

Continuous fibre-reinforced thermoplastic acrylic-matrix composites prepared by liquid resin infusion – a review

Winifred Obande, Conchúr M. Ó Brádaigh, and Dipa Ray*

School of Engineering, Institute for Materials and Processes, The University of Edinburgh, Sanderson Building, Robert Stevenson Road, Edinburgh EH9 3FB, Scotland, United Kingdom.

*Corresponding author. *Email address*: dipa.roy@ed.ac.uk

Abstract:

Increasing demand for lightweight materials is a major driving force for the steady growth of the continuous fibre-reinforced polymer composite industry. In recent years, strict global targets demanding greater environmental responsibility have led to a shift in research focus to address the end-of-life challenges posed by the use of thermoset matrices. Thermosets offer lower-cost processibility than thermoplastics, which historically required cost- and energy-intensive production methodologies. Consequently, despite their well-demonstrated recyclability, thermoformability and weldability, thermoplastics are yet to attain the same technological maturity as thermosets. *In situ* polymerisable thermoplastic resins have been identified as attractive emerging solutions for improving the processibility of thermoplastics. Thus, are essential materials in meeting the demand for fibre-reinforced thermoplastic composites. This review presents a comprehensive summary of recent works on room-temperature-processible liquid thermoplastic acrylic resins and their composites. Moreover, open problems and research opportunities are identified and discussed.

Keywords: A. Polymer-matrix composites (PMCs), A. Thermoplastic resin, B. Mechanical properties, E. Liquid composite moulding

1 Introduction

In parallel to the increasing demand for fibre-reinforced polymer (FRP) composites, there is renewed interest in thermoplastic (TP) matrices across many sectors where their thermoset (TS) counterparts are dominant. While it has long been established that TP matrices offer more favourable benefits than TS matrices in terms of recyclability, welding and thermoformability [1–3], their high-melt viscosities

necessitate high processing temperatures and pressures, and thus, renders them cost-prohibitive and impractical for most sectors [4,5]. Research efforts to address this have paved the way for the application of innovative *in situ* polymerisation methodologies for the production of continuous fibre-reinforced TP composites. Early-generation reactive TP precursors such as cyclic butylene terephthalate (CBT) [6–10], caprolactam [11,12] and laurolactam [13,14] now facilitate the production of fibre-reinforced polybutylene terephthalate (PBT), polyamide-6 (PA-6) and polyamide-12 (PA-12) by liquid composite moulding, respectively. These materials do, however, require mould heating to achieve temperatures above 150°C (PA-6 and PA-12) and 180°C (PBT), which makes the fabrication of large-scale structures relatively challenging. This additional requirement for mould heating may be impracticable for the wind energy sector, for instance, where blade lengths continue to increase to meet growing global demand [15–17].

The study of bulk polymerization of acrylic resins started in the 1940s, and only few studies were reported on the reactive processing of acrylic composites [18]. The growing interest in the field of TP-FRPs has led to the development of Elium®, a family of liquid TP acrylic resins, which are suitable for manufacturing large composite structures with continuous fibre reinforcement at room temperature via *in situ* polymerisation. With viscosities as low as 100 mPa.s, these acrylic resins are considered more cost-effective than the aforementioned first-generation reactive resins. Moreover, their suitability for the production of large-scale components by resin infusion [19–21]; and their thermoformability and recyclability [22] have recently been demonstrated.

The present article reviews the advancements to-date in the use of reactive acrylic resins as attractive solutions to the challenges associated with traditional thermosetting and thermoplastic matrices for composite applications. Published works on the mechanical and thermomechanical performance of *in situ* polymerisable acrylic matrices and their composites are reviewed and discussed in this article. A comprehensive summary of comparative analyses performed to-date alongside comparable thermosetting composites is also presented. This article is intended for the composites community, so a detailed description of the polymerisation chemistry of the acrylic resins has not been included within the scope of this article. In the sections that follow, new name assignations have been applied as detailed in Table 1; e.g.: the use of E-150 now implies Elium® 150.

Table 1. Summary of the resins in the works under review and new name assignations,with unreinforced matrix properties..

Commercial name	Elium® 150	Elium® RT150	Elium® 180	Elium® 188, Elium® 188 O	Elium® 280	Elium® C595 E
New name assignation	E-150	E-RT150	E-180	E-188O	E-280	E-C595E
Recommended process	Infusion	Injection	Infusion; injection	Infusion; injection	-	Pultrusion; wet compression; winding
Viscosity at 25°C (m.Pas)	100	100	100	100	-	500
Process temp. (°C)	15 – 25	15 – 25	20 – 60	20 – 60	-	20-115
Process time @ 25°C (min)	55 – 60	55 – 60	45 – 60	45 – 60	-	Adjustable
Initiator/Catalyst	Dibenzoyl peroxide	Dibenzoyl peroxide	Dibenzoyl peroxide	Dibenzoyl peroxide	-	Peroxide blend
Tensile strength (MPa)	76	76	66	66	76	66
Tensile modulus (GPa)	3.3	3.3	3.17	3.17	3.3	3.17
Elongation (%)	6	6	2.8	2.8	6	-
Compressive strength (MPa)	130	130	116	116	-	-
Compressive modulus (GPa)	-	-	3.83	3.83	-	-
Flexural strength (MPa)	130	130	111	111	-	-
Flexural modulus (GPa)	3.25	3.25	2.91	2.91	-	-

2 Polymerisation reaction of liquid reactive acrylic resins

2.1 Studies on polymerisation behaviour

Acrylics polymerise by free radical polymerisation and undergo the three characteristic reactions: (i) Initiation is typically brought about by radical peroxides (initiators or catalysts), which comprise unpaired electrons that open double bonds (unsaturation) in the monomers, resulting in the creation of reactive radical sites on the monomers; (ii) The chain propagation reaction ensues, with unreacted monomer molecules successively being 'captured' and newly unpaired electrons becoming available at growing chain ends; (iii) Termination can subsequently occur by recombination, usually in the presence of another radical, or a termination agent to bring growth to an end. Process parameters such as initiator concentration, temperature and pressure, have been reported to significantly influence the rates of radical polymerisation reactions and consequently, the resultant molecular weight and molecular weight distribution [23,24]. Understanding their effects on the resulting acrylic polymer system is an essential step in fostering an established knowledge base on optimum processing conditions. Presented herein, is a brief overview of published works on polymerisation behaviour of acrylics as a function of processing conditions.

2.1.1 Influence of initiator content

Using the E-150 grade of liquid acrylic resin and a commercial organic peroxide, it was reported that initiator content influences the reaction stages of free radical polymerisation [25]. Both high (1.6 %) and low (0.8 %) initiator contents promote slower initiation and termination reaction rates than an intermediate concentration (1.2 %). Combined with higher onset temperatures (75°C) for the high and low concentrations, and lower temperature (58°C) for the intermediate concentration, the authors concluded that these observations were associated with the availability of the radical species provided by the initiator. It was suggested that at the lower radical concentration (0.8 %), fewer acrylic monomer molecules were initiated and thus, the growth of a few long chains culminated in the observed behaviour. In contrast, higher concentration (1.6 %) promoted concurrent growth of several short chains. It can thus be deduced that in all cases, these effects are combinatory effects of the competitive chain growth and ultimate termination reactions. Interestingly, the lowest initiator content was found to cause an instantaneous, exponential increase in viscosity up to the terminal cycle temperature (rheological study). Increasing the initiator content was reported to reduce the viscosity at all polymerisation reaction stages.

A positive correlation exists between the initiator content and glass transition temperature (Figure 1), with equivalent values reported for 1.2 % and 1.6 % concentrations [25]. While no effects were observed on tan delta peak amplitudes between the samples containing 0.8 % and 1.2 % of initiator content, a pronounced increase was observed for the sample polymerised with 1.6 wt. % of the initiator. These differences were reported to be related to differences in polymer chain lengths between the samples.

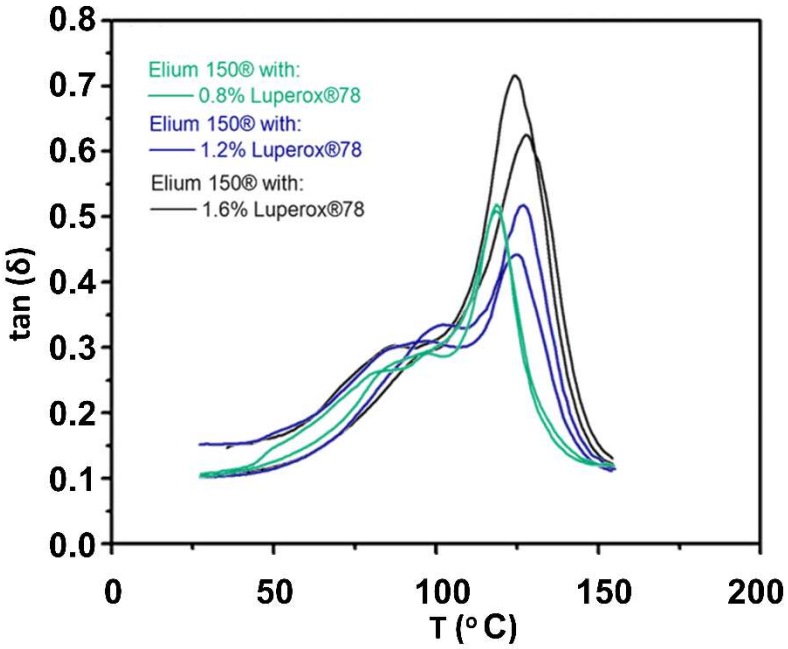

Figure 1. Dynamic-mechanical analysis results showing effect of initiator contents of (a) 0.8 %, (b) 1.2 %, and (c) 1.6 % on tangent delta (tan (δ)) as a function of temperature (T) (Copyright permission from Wiley. Adapted from Figure 7 in [25]).

The same authors reported no major effects of initiator content on the thermal degradation behaviour on polymerised samples. All samples were reported to undergo two mass loss stages, evidenced by the two valleys in the derivative thermogravimetric (DTG) curves (Figure 2). For samples polymerised using initiator contents of 0.8 %, 1.2 % and 1.6 %, respectively, the valleys are as follows. (i) *Valley 1*: occurred at 113°C, 115°C and 108°C, and was said to be related to the depolymerisation of head-to-head linkages (from recombination termination reactions) and residual monomers. (ii) *Valley 2*: occurred at 298°C, 302°C and 326°C. This valley was said to be associated with random scission. Evidently, an increase in initiator content promoted the formation of more head-to-head linkages. Finally, a third characteristic decomposition valley, which is observed for acrylic-based polymers due to the decomposition of unsaturated chain ends

at temperatures of around 230°C was said to be absent due to copolymerisation with oxygen during the polymerisation process.

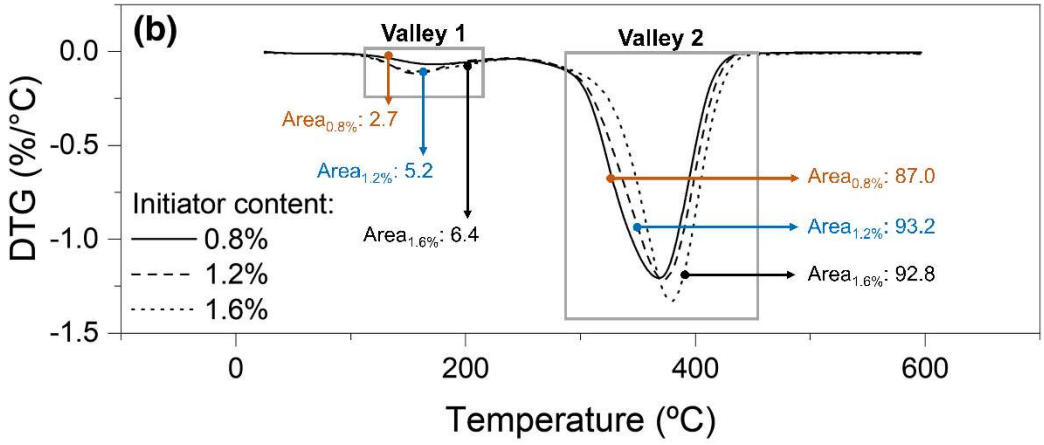

Figure 2. Results of the thermogravimetric analyses on samples polymerised with initiator contents of 0.8 wt. %, 1.2 wt. % and 1.6 wt. %. Valleys corresponding to the first and second mass loss events are marked as 1 and 2, respectively (Copyright permission from Wiley. Adapted from Fig. 8 in [25]).

On the influence of initiator content on the degree of conversion, the samples containing 0.8 wt. % and 1.6 wt. % of initiator appear to exhibit slower initiation and propagation rates as shown in Figure 3 [25].

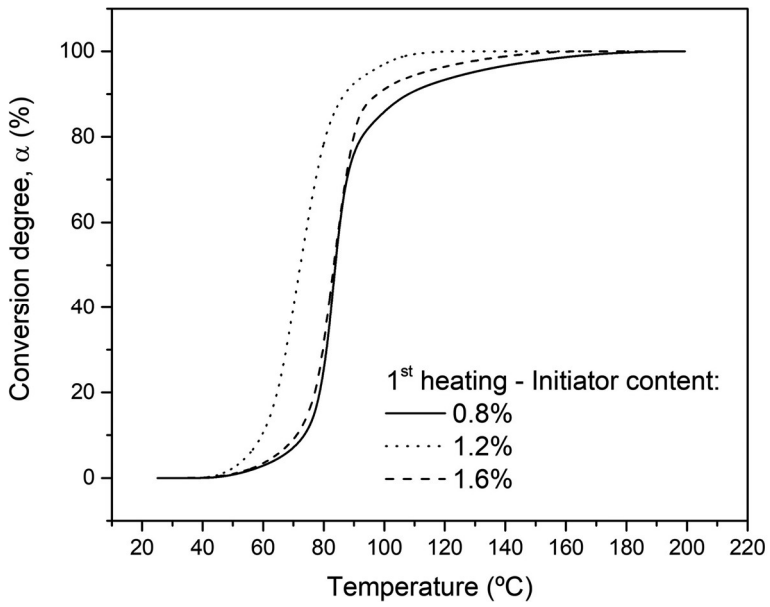

Figure 3. Degree of conversion as a function of temperature for E-150 samples polymerised with 0.8 wt. %, 1.2 wt. % and 1.6 wt. % of initiator (Copyright permission from Wiley [25]).

The work by de Andrade Raponi et al. [25] provides an understanding of the influence of initiator content for E-150 resin; key findings are summarised in Table 2.

Table 2. Summary of critical findings on the influence of initiator content on polymerisation behaviour of liquid acrylic resins. Data sourced from [25].

	Polymerisation				*Rheology*	*Glass transition*	*Decomposition*	
Initiator content (wt. %)	$T_{100\,\%}$ *(°C)*	T_{onset} *(°C)*	T_{max} *(°C)*	$-\Delta H$ *(J/g)*	T_{gel} *(°C)*	T_g *(°C)*	T_{onset} *Peak 1 (°C)*	T_{onset} *Peak 2 (°C)*
0.8	199.3	75.9	82.6	129.4	87.0	116.2	113	298
1.2	122.4	57.9	70.4	150.7	84.4	123.4	115	302
1.6	163.9	74.0	81.8	210.7	87.5	123.3	108	326

While this is an essential study in advancing knowledge on the behaviour of E-150, it is worth noting that compositional differences exist between the grades of this novel family of acrylic resins. As such, research attention towards understanding the effects of initiator content for other grades of Elium® is essential.

2.1.2 Influence of temperature

The polymerisation of first-generation acrylate monomers has been shown to be influenced by temperature due to effects on the polymerisation time, the formation of voids, and the risk of exothermic runaways [18]. de Andrade Raponi et al. [26] showed that temperature significantly influences the termination step of polymerisation reactions for unreinforced E-150 containing 1.2 % of a commercial organic peroxide, and invariably, its degree of conversion. A key contribution of this work was the proposal of a three-stage thermal processing cycle (Figure 4a) comprising sequential isothermal segments at 25°C (25 min), 80°C (30 min) and 110°C (120 min), with heating rates of 4°C/min.

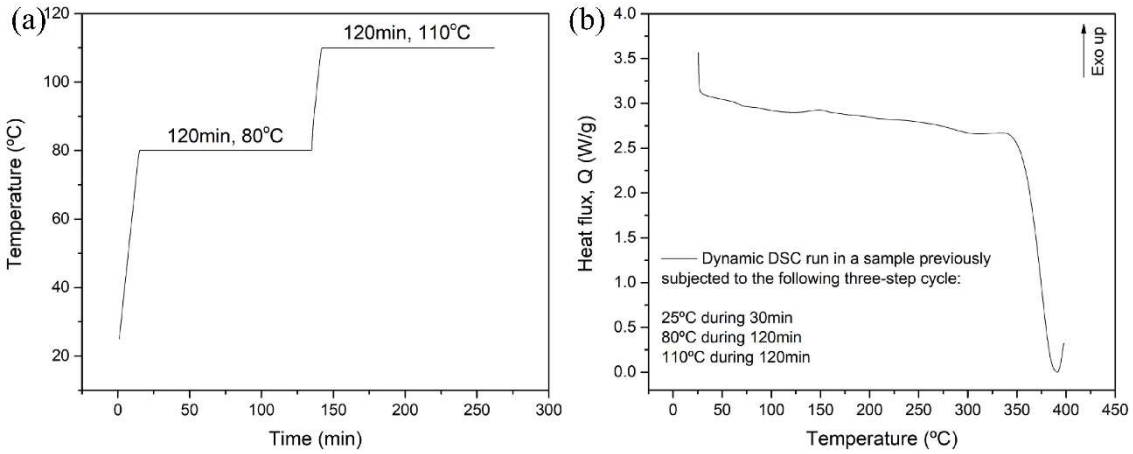

Figure 4. An (a) optimised three-step thermal cycle for E-150 resin and (b) DSC validation results for the cycle as developed by de Andrade Raponi et al. [26] (Copyright permission from Elsevier. From Figs. 9 & 10 in [26]).

The first segment was employed to promote a slow reaction rate to limit the formation of thermally-induced voids. DSC analysis on the polymerised sample (Figure 4b) revealed no exothermic peak; no further polymerisation was detected. As with the work reviewed in 2.1.1, an obvious limitation is that this study focused solely on process optimisation for this specific grade of acrylic resin, and the proposed process parameters may not be directly applicable to other grades given the compositional variations that may exist in this family of acrylic resins. Thus, further studies of this nature covering several grades may prove beneficial. Interestingly, the manufacturer remarks on the suitability of this resin grade for room-temperature polymerisation, however, suggests a post-polymerisation heating step at 80°C for 4 h to realise enhanced mechanical performance [27].

2.1.3 Polymerisation exotherm

Murray et al. [28] reported the need for a proprietary exothermic control agent for the production of thick sections of glass fibre-reinforced acrylic laminates. Murray et al. [19] highlighted the need for such measures in the production of thick components (>12 mm). These findings are supported by Charlier et al. [29] who reported constant heat flow and reaction rate up to 40 % conversion, followed by an instantaneous increase in reaction rate up to 100 % conversion. This rate change was believed to be attributed to an auto-acceleration phenomenon (the gel effect), reported to induce a high degree of exotherm in bulk free radical polymerisation. Peak exotherm temperatures of 45°C [30] and 77-90°C [22] have been reported for thin

and thick sections, respectively. An increase in laminate thickness from 3.8 mm to 11.3 mm has been shown to result in a corresponding increase in peak exotherm temperature of 21.5°C [31].

3 Fabrication of continuous fibre-reinforced acrylic-matrix composites

Most published works on the properties of *in situ* polymerised acrylic-matrix composites have employed a liquid resin infusion technique [32–37]; however, resin transfer moulding (RTM) [34,38–40], wet lay-up and press moulding [41] have also been used.

Depending on the variant of liquid resin infusion method used (such as those in Hindersmann's overview [42]), an array of auxiliary materials are used to aid liquid resin infusion and the subsequent release or demoulding process. In most cases, the set-up shown in Figure 5 is employed, where a flexible membrane or bag is used in conjunction with a rigid tool base. Traditional liquid resin infusions are typically preceded by a resin degassing process for the removal of dissolved gases and micro-bubbles within liquid resins such as epoxy [43].

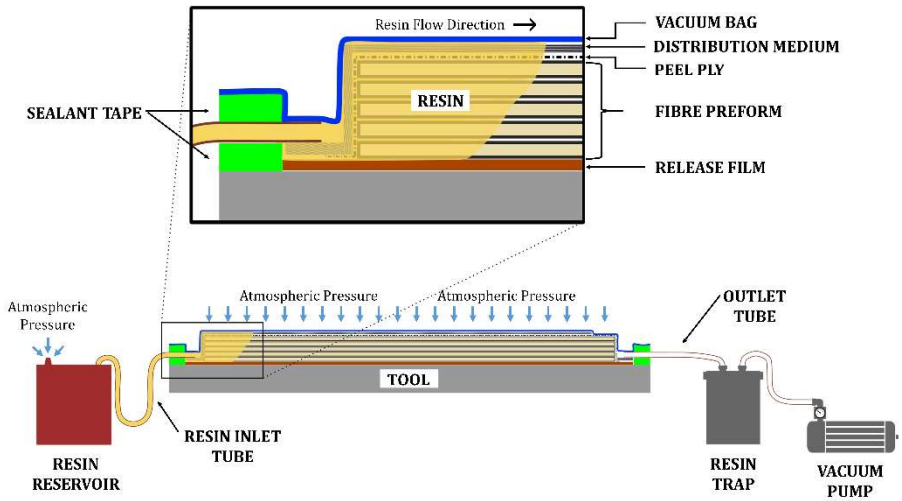

Figure 5. Conventional liquid resin infusion process under a flexible membrane set-up.

However, the short pot life and infusion window (~ 40 min) of these acrylic resin systems makes degassing impractical. Where it has been attempted on E-280, no significant benefits were reported [33]. With the exception of the work done by Cousins et al. [22], no authors reported a resin degassing step for acrylic-based laminates. Across most of the reviewed works, a conventional liquid resin infusion configuration with a flexible membrane was employed. Additionally, vacuum RTM (VRTM) or RTM Light was also

reported using an innovative adjustable-thickness tool (Figure 6) with two rigid mould halves [37,44], where vacuum is used for both clamping and resin flow [42].

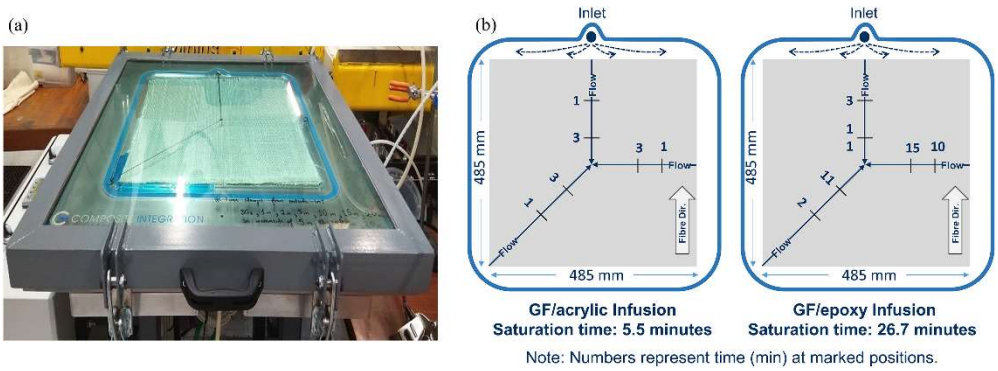

Figure 6. (a) Composite Integration liquid resin infusion equipment and (b) graphical representation of flow fronts during the fabrication of glass fibre-reinforced acrylic and epoxy laminates (Copyright permission from Elsevier. From Fig. 1 in [37]).

A two-stage technique for the fabrication of flax fibre-reinforced acrylic was reported by Baley et al. [41]. (i) The initial manual impregnation stage produced fully wetted-out preforms, which were subsequently (ii) hot-press moulded for enhanced void-elimination and consolidation. While this resin grade (E-150) does not require heating during the polymerisation process [27], the use of heat during and after the polymerisation step is reported by the authors as manufacturer's recommendations. Heating was also employed by Boufaida et al. [40] for RTM fabrication of acrylic-based laminates; however, this was reported by the authors as a requirement to thermally activate the polymerisation process due to the incompatibility of the fibre sizing on the reinforcements employed with the intrinsic activation agent in the initiator. It was suggested that the activator within the initiator reacted with the epoxide groups within the multi-compatible sizing formulation. Thus, thermal activation was required in-lieu of chemical activation. While the precise grade of acrylic resin used was not specified in the work by Boufaida et al. [40], the suitability of the RTM process for producing acrylic-matrix laminates has also been demonstrated by Bhudolia et al. [34] using E-280 with carbon fibre reinforcements (with a thermoplastic-compatible sizing agent). Table 3 presents an overview of the most adopted fabrication processes of acrylic matrix composites and the laminate quality achieved by resin grade and fibre type.

Table 3. Summary of reported processing techniques of acrylic matrix composites and resulting fibre (V_f) and void (V_v) volume fractions, by resin grade and fibre type.

Reinforcement	*Resin*	*Process*	V_f *(%)*	V_v (%)	*Reference*
Carbon	E-280	i. Liquid resin infusion ii. RTM	i. 48 – 60 ii. 57	i. 0.1 – 1 ii. N/S	i. [33,35,57,63] ii. [34]
Carbon	E-150	i. Hand layup & vacuum moulding† ii. Liquid resin infusion	i. N/S ii. N/S	i. N/S ii. N/S	i. [106] ii. [58]
Carbon	N/S	Liquid resin infusion	60	N/S	[65]
Glass	E-180, E-188 O	i. Liquid resin infusion ii. VRTM	47-49.5	0.4	[37,51]
Glass	E-150	Liquid resin infusion	N/S	N/S	[54]
Glass	N/S	Liquid resin infusion	i. 54.2 ii. 46.5 iii. 52.4	i. N/S ii. 7 iii. 1.3	i. [28] ii. [36] iii. [45]
Flax	E-RT150	i. Hand layup & press moulding ii. Liquid resin infusion	i. 48 ii. 35 – 40	i. N/S ii. 2.5 – 7.5	i. [41] ii. [107]
Flax	N/S	Liquid resin infusion	37.1	5	[45]

†**:** thermally post-processed, **N/S:** Not specified

4 Properties of acrylic-matrix composites

4.1 Glass fibre-reinforced acrylic-matrix composites

4.1.1 Tensile properties

Lorriot et al. [36] reported comparable longitudinal tensile strengths (~860 MPa) and moduli (40 GPa) in glass fibre-reinforced acrylic and epoxy laminates, reporting marginally higher (5 %) failure strain in the acrylic-based composite. Similar comparability was reported by Chilali et al. [45]. However, despite a relatively high fibre volume fraction (~52 % for the acrylic-based material), the reported tensile strength (380 MPa) and modulus (23 GPa) are considerably lower than indicated by other authors. Cousins [46] identified a marked superiority in the tensile strength of an acrylic composite over its epoxy counterpart, reporting strengths of 916 MPa and 723 MPa, respectively for both materials. Even higher longitudinal tensile strength (1241 MPa) and modulus (52.7 GPa) were reported by Zoller et al. [47], possibly owing to higher fibre weight fractions (81 %), the use of a different grade of acrylic resin (E-C595E) or the effects of the pultrusion process on fibre alignment. Obande et al. [37] characterised the tensile properties of acrylic- and epoxy-based glass FRPs and reported marked superiority in transverse strength for the acrylic system; strengths of 73 MPa and 54 MPa were reported, respectively. Equivalent transverse tensile moduli were reported for both materials at 13 GPa. As shown in Figure 7, the authors reported distinct failure characteristics in both materials. The stress-strain behaviour (Figure 7b) for the epoxy-matrix composite showed an earlier onset of non-catastrophic damage; the authors suggested a link between this behaviour and the multiple transverse cracks observed on test samples (Figure 7a). These were shown to accumulate along the sample gauge length during loading up to failure. This phenomenon was not reported for acrylic-based samples; rather, fibre splitting along the loading direction was evident. These were identified as originating from 90° reinforcing yarns in the fabric.

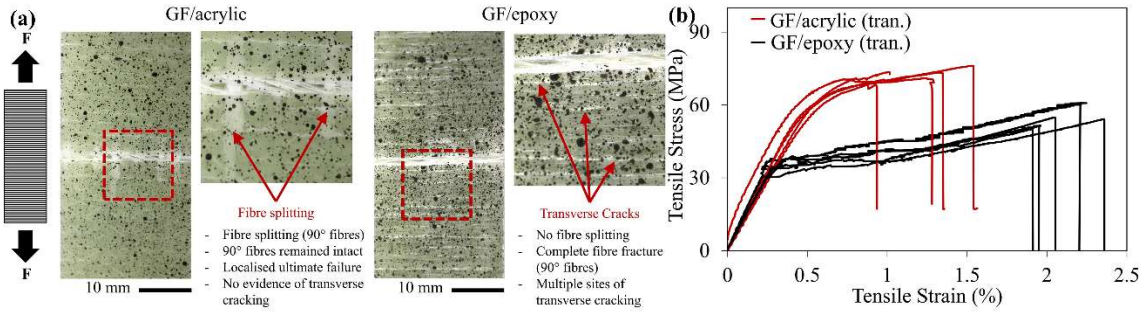

Figure 7. (a) Macroscopic failure behaviour and (b) stress-strain responses of glass fibre-reinforced acrylic and epoxy composites subjected to transverse tensile loading (Copyright permission from Elsevier. Reproduced from Figs. 2 & 3 [37]).

4.1.2 Compressive properties

The compressive performance of glass fibre-reinforced acrylics has not been extensively studied. Cousins [46] comparatively assessed glass fibre-reinforced acrylic and epoxy composites and reported equivalent strengths (~600 MPa) and moduli (~34 GPa) for both materials. Substantially higher average compressive strength (1044 MPa) and modulus (~52 GPa) values were reported for pultruded glass fibre-reinforced acrylic based on E-C595E E by Zoller et al. [47]. While no details of fibre volume or mass fractions were provided for the materials reported by Cousins [46], the high fibre mass fraction of 81 % reported by Zoller et al. [47] possibly explains the high compressive strength and modulus. Besides, the use of the pultrusion process may confer a high degree of fibre alignment, which are known to influence the longitudinal compressive performance of composites [48]. To the best of our knowledge, no other works focus on assessing the compressive performance of glass fibre-reinforced acrylic composites. The lack of published literature on this area highlights the need for more benchmarking studies on the compressive properties of glass-reinforced acrylic composites alongside more traditional thermoset matrix-based composites.

4.1.3 Flexural properties

Cousins [46] measured higher flexural strengths in the acrylic-based composite (1006 MPa) than the epoxy-based reference material (809 MPa); the authors reported moduli of values of ~37.5 GPa and ~35 GPa, respectively. No fibre volume fractions were reported for these materials. As with the tensile and compressive properties in Sections 4.1.1 and 4.1.2., Zoller et al. [47] showed that it was possible to achieve high-flexural-performance glass fibre-reinforced acrylics based on E-C595E E by pultrusion. The average

longitudinal flexural strength and modulus for this material were 1291 MPa and 44.7 GPa, respectively. Davies and Arhant [49] reported flexural strengths of 703 MPa and 606 MPa, and moduli of 40.1 GPa and 38.2 GPa for glass fibre-reinforced acrylic and epoxy composites with fibre volume fractions of 52 and 53 %, respectively. These trends were also observed by Obande et al. [37], who reported strengths of 879 MPa and 869 MPa, and moduli of 40 GPa and 38 GPa for glass fibre-reinforced acrylic and epoxy composites, with fibre volume fractions of 49.5 %, respectively. In the same study, the authors reported the opposite trend for transverse flexural performance, reporting strengths of 91 MPa and 94 MPa and moduli of 11 GPa and 12 GPa for the acrylic- and epoxy-based materials. Interestingly, despite possessing consistently higher longitudinal characteristics than composites produced from other grades of the acrylic resin and produced using other techniques, the material studied by Zoller et al. [47], exhibited inferior transverse flexural strength (68.9 MPa) and marginally higher modulus (11.5 GPa) than that reported by Obande et al. [37].

4.1.4 Shear properties

In-plane shear properties of a glass fibre-reinforced acrylic matrix and an epoxy-based counterpart were studied by Lorriot et al. [36]. The authors reported higher shear modulus (~31 %) in the epoxy-matrix composite and comparable shear strengths in both materials. Chilali et al. [45] reported comparable performance during in-plane shear strengths, with both acrylic- and epoxy-matrix composites yielding strengths of ~68 MPa and moduli or ~6 GPa. Cousins [46] found that an acrylic-based FRP possessed 8 % lower short-beam shear strength than its epoxy-based counterpart, reporting strengths of ~50 MPa and 54 MPa, respectively. Obande et al. [37] also studied the short-beam shear behaviour of glass fibre-reinforced acrylic and epoxy composites and reported comparable shear strengths in both materials, with the acrylic-based composite being marginally higher at 58 MPa (+2 %) than its epoxy counterpart. Dissimilar damage evolution was described by the authors, who found that epoxy-matrix samples exhibited a more pronounced onset of failure beyond load peaks, dropping by up to 30 % from the peak load. In contrast, a smoother and more gradual drop in load was observed with acrylic samples. For unidirectional glass-fibre reinforced acrylics, Davies and Arhant [49] reported 21 % higher short-beam shear strengths than a comparable epoxy-based composite. Despite the authors exploiting specialised acrylic-compatible sizing on their reinforcements, an average short-beam shear strength of 46 GPa was reported for the acrylic-based samples. The grade of acrylic resin used in this work (E-180) and that was used by Obande et al. [37], E-188 belong

to the same family of resins [50] and as such, should exhibit similar performance for the same type of reinforcement. Moreover, short-beam shear behaviour should ideally be enhanced in work by Davies and Arhant [49], particularly given the benefits that specialised sizing formulation potentially confer and marginally higher fibre volume fraction (52 %) than that reported by Obande et al. [37] (49.5 %). While these authors employed different stacking sequences, these observations highlight the need for comparative benchmarking studies on sizing technology for these acrylic matrices.

4.1.5 Impact properties

Obande et al. [51] comparatively assessed the drop-weight impact behaviour of glass fibre-reinforced acrylic composites with an epoxy-based reference. Following impact events at 15 and 30 J, the authors measured the resultant damage area as shown in Figure 8 to assess impact damage resistance. Expressing average damage area as percentages of the total sample face area in acrylic- and epoxy-based materials, 15 J impact events produced damage areas of 4.4 ± 0.9 % and 3.9 ± 0.3 %, respectively, whereas, 30 J impacts resulted in 7.4 ± 0.5 % and 6.6 ± 0.5 %, respectively. From these findings, it was concluded that the reference epoxy-based material sustained a lesser extent of measurable damage, and thus, was deemed more damage resistant than the acrylic-based composite at the energy levels used in the study. Kinvi-Dossou et al. [52] conducted a similar study and although the authors did not quantify the extent of impact-induced damage, their study ranked acrylic-matrix composites more damage resistant than its polyester- and epoxy-based counterparts.

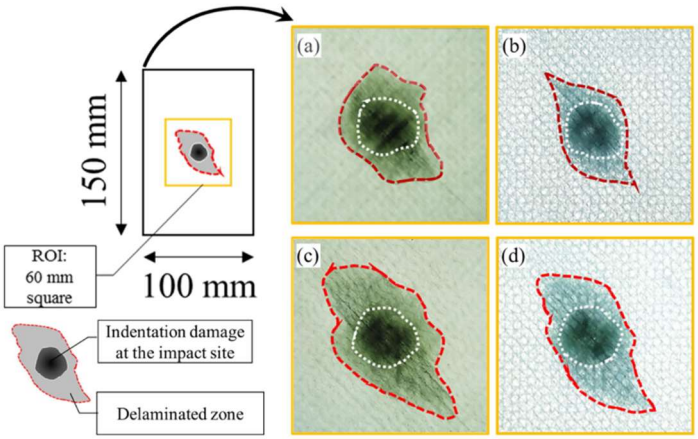

Figure 8. Representative damage states for glass fibre-reinforced (a) acrylic at 15 J, (b) epoxy at 15 J, (c) acrylic at 30 J, and (d) epoxy at 30 J. ROI: region of interest (Copyright permission from Elsevier. Adapted from Fig. 2 in [51]).

As shown in Figure 9, the damaged envelope grows considerably for the polyester- and epoxy-matrix composites, with evidence of gross delamination being observable. Only minimal damage states are presented for the acrylic composite samples at these energy levels. The authors believe that the superior impact strength is attributed to improved interfacial adhesion between the glass fibres and the acrylic matrix, but provide no strong evidence to support this claim. In addition, the impact performance of the acrylic laminate was also reported to be enhanced by shear banding within the matrix, which contributes to the dissipation of bulk strain energy and gives way to shear localisation. A further remark by the authors suggests that this acrylic is considerably more ductile than the epoxy and polyester matrix, which are described as brittle. However, acrylics have been shown to possess low failure strain and strain-dependent embrittlement [37,51,53] as brittle amorphous thermoplastic materials.

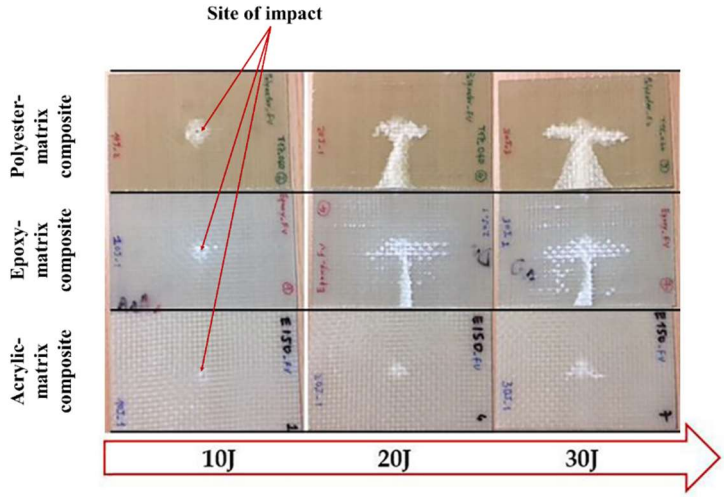

Figure 9. Impact-face damage states on glass fibre-reinforced polyester, epoxy and acrylic composites subjected to impact events of 10 J, 20 J and 30 J (Copyright permission from Elsevier. Adapted from Fig. 8 in [52]).

However, it is worth noting that woven reinforcement was used in the study by Kinvi-Dossou et al. [52], whereas Obande et al. [51] presented results for a quasi-isotropic laminate. Cadieu et al. [54] assessed the effects of rate on the out-of-plane loading response of glass fibre-reinforced E-150 using quasi-static indentation and drop-weight impact; it was concluded that higher loading rates result in lower penetration depth and higher stiffness, which results in higher elastic energy and conversely, lower dissipated energy.

At low impact energies and low indentation, no rate effects were reported for the area of the damaged zone. At higher energy levels, however, a more substantial reduction is observed in the damaged area at the shorter timescale. Damage mechanisms were not found to be affected by the loading rate; the authors observed delamination, matrix cracking and fibre-related failure at all loading rates.

4.1.6 Interlaminar fracture toughness

4.1.6.1 Mode-I interlaminar fracture toughness

Obande et al. [37] showed that glass fibre-reinforced acrylic laminates exhibited superior (+15 %) Mode-I interlaminar fracture toughness than their epoxy-based counterparts. As shown in Figure 10, the acrylic composite also possessed higher (+19 %) initiation fracture toughness.

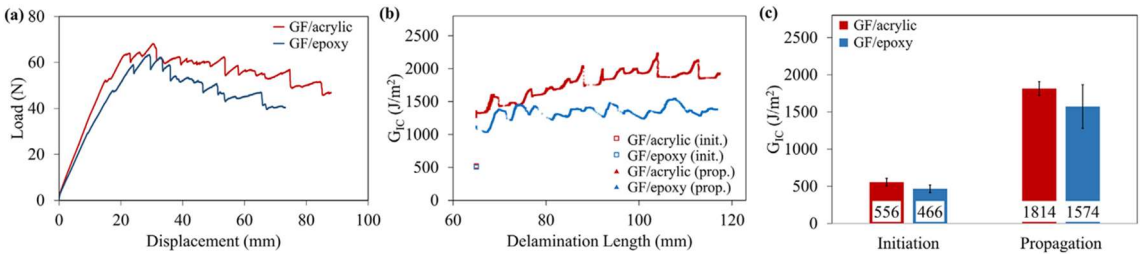

Figure 10. (a) Load-displacement curves and (b) resistance curves (R-curves) for glass fibre-reinforced acrylic and epoxy composites, and (c) initiation and propagation fracture toughness values of same (Copyright permission from Elsevier. From Fig. 12 in [37]).

Progressive unstable delamination growth was reported by the authors, with evidence of stick-slip propagation mechanisms observed. From the higher slope of the R-curve for the acrylic-based sample in Figure 10b, the authors reported the superiority of the thermoplastic acrylic composite in damage resistance over its epoxy counterpart. Both materials exhibited some extent of fibre bridging at the crack tip, as shown in Figure 11; however, this was more prominent in the acrylic-matrix composite. In terms of fractographic behaviour, the presence of distinctly ductile characteristics was reported in the case of the acrylic-matrix composite, with more brittle features being observed on the epoxy composite. They also remark on the likelihood of tow-rupture and debonding occurring along the interface of these 90° tows, which would inadvertently be pathways for damage-related energy absorption. As such, the results presented were not deemed representative of unidirectional fracture behaviour. With the exception of this work, no other

authors have reported findings on the Mode-I interlaminar fracture behaviour of glass fibre-reinforced acrylic composites, highlighting the need for further exploration of this topic for these materials.

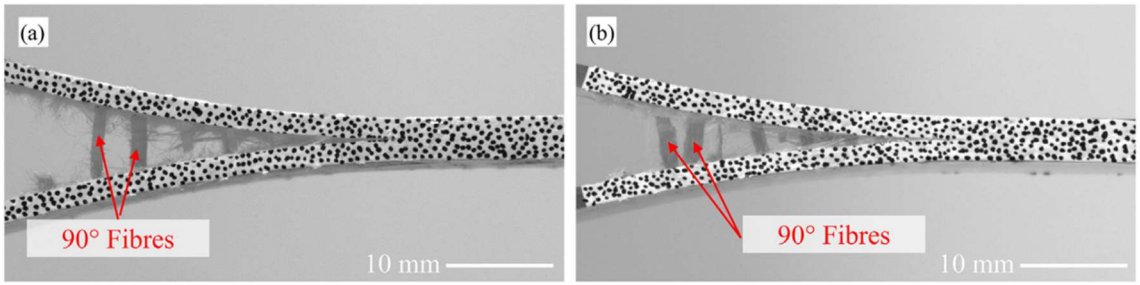

Figure 11. Delamination behaviour of glass fibre-reinforced acrylic and epoxy samples undergoing double cantilever beam testing at equivalent test times (Copyright permission from Elsevier. From Fig. 13 in [37]).

4.2 Carbon fibre-reinforced acrylic-matrix composites

4.2.1 Tensile properties

The tensile properties of cross-ply carbon acrylic and epoxy FRPs were studied by Bhudolia et al. [35]. While localised brittle fractures were observed in the epoxy-based material, fibre splitting and fracture, and delamination were reported as the predominant modes in the acrylic-based FRP. Ultimately, the epoxy material had superior strength (1217 MPa) and modulus (66.7 GPa) than its thermoplastic counterpart, which had corresponding values of 1004 MPa and 53.1 GPa. A major limitation of this study is that dissimilar carbon reinforcement systems were used, making it challenging to draw definitive conclusions. Interestingly, Davies and Arhant [49] reported lower tensile strength (831 MPa) and higher modulus (71.9 GPa) for thick-ply carbon fibre-reinforced acrylic composite.

4.2.2 Flexural properties

The flexural properties of an acrylic-based material were comparatively evaluated alongside a baseline epoxy system. In this work, Bhudolia et al. [35] reported 33.3 % and 9.5 % higher strength and modulus values, respectively for the epoxy FRP, which failed on both the tensile and compressive sides. However, only compressive failure was observed in the acrylic composite, which had average strength and modulus values of 671.1 MPa and 52.1 GPa, respectively. These findings were, however, affected by the ply configuration in each laminate – conventional thick-ply non-crimp fabric (NCF) was used in the fabrication of the acrylic laminate, whereas its epoxy-based counterpart contained thin-ply NCF reinforcement.

In another work by Bhudolia et al. [55], the authors presented findings on flexural behaviour of thin-ply carbon fibre-reinforced acrylic and epoxy composites. Using quasi-isotropic laminates with fibre volume fractions of 58.3 % and 60 %, respectively, the authors reported flexural strengths of 813 MPa and 835 MPa for the acrylic- and epoxy-based materials, respectively. Their moduli were found to be comparable at ~51 GPa. Differences in failure behaviour were highlighted. For thick-ply laminates with similar stacking sequence, Davies and Arhant [49] reported lower mean flexural strength (590 MPa) and higher modulus (103 GPa). Figure 12 shows the failure characteristics reported by Bhudolia et al. [55]. A greater extent of visible matrix deformation on the side in compression was reported for the acrylic-based composite; delamination was observed in its epoxy counterpart.

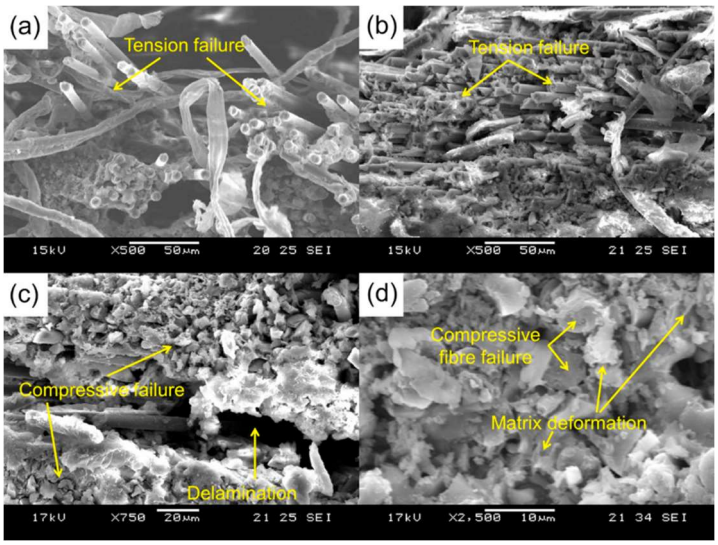

Figure 12. Scanning electron micrographs showing flexural failure modes of thin-ply carbon fibre-reinforced (a) & (c) epoxy and (b) & (d) acrylic composites (Copyright permission from Elsevier. From Fig. 2 in [55]).

This work also represents the first implementation of annealing for this family of acrylic resins. Although similar to the post-processing cycles recommended by the manufacturers for some grades of Elium® resin, it was performed in a hot press (80°C for 2 h) as opposed to a free-standing heating cycle. This annealing process was said to facilitate targeted microstructural reorganisation, a more complete polymerisation reaction, enhanced matrix ductility and interfacial adhesion as shown in Figure 13. The grade of Elium® under consideration in this work was not disclosed, which indirectly limits the transferability of the findings

presented therein to other grades. It is unclear if the insufficient polymerisation was associated with sizing effects as previously suggested by Boufaida et al. [40].

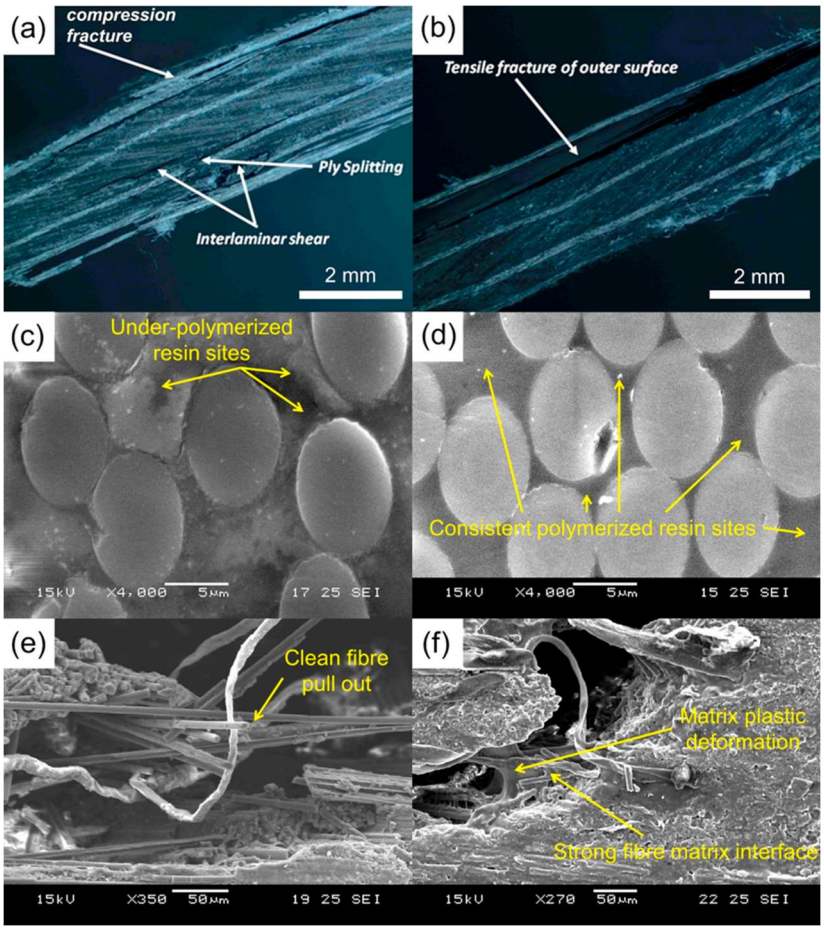

Figure 13. Flexural failure modes of thin-ply carbon fibre-reinforced acrylic composites: (a), (c) & (e) without annealing; and (b), (d) & (f) with annealing (Copyright permission from Elsevier, From Fig. 3 in [55]).

4.2.3 Impact properties

Carbon fibre-reinforced acrylic composites have been shown to possess superior structural integrity during impact compared to an equivalent epoxy-based composites. The acrylic-matrix composite was reported to be capable of undergoing more elastic deflection before the maximum impact load was reached [34]. The authors also reported strain sensitivity in this material, with increasing energy levels giving rise to greater elastic-plastic deformations relative to the epoxy-matrix composite. This had direct consequences on the

resulting damage states of both materials (Figure 14 and Figure 15); a larger extent of delamination and catastrophic failure characteristics were observed in the carbon fibre-reinforced epoxy samples for 42-J and 52-J impacts. Interestingly, impacts at a lower energy level (25 J) appeared to produce more severe and extensive damage states in the acrylic-based material such as fibre fractures and interlaminar cracking (Figure 15a); delamination and tensile failure of back-face plies can be seen for the epoxy-matrix composite (Figure 15d). The authors also suggested that plastic zone development at the tips of interlaminar cracks contributed positively to enhancing the ductility of the acrylic-matrix composite. It was also proposed that shear crack propagation was favoured by superior interfacial strength in the carbon fibre-reinforced acrylic material. In a similar study, the use of thin-ply carbon fibre reinforcement has also been shown by Bhudolia et al. [56] to produce more impact damage-resistant acrylic-matrix composites than is possible with standard thick-ply reinforcement. Thin-ply carbon fibre-reinforced acrylic composites were found to exhibit more favourable elastic-plastic deformation, leading to smaller delamination zones than in the thick-ply variant.

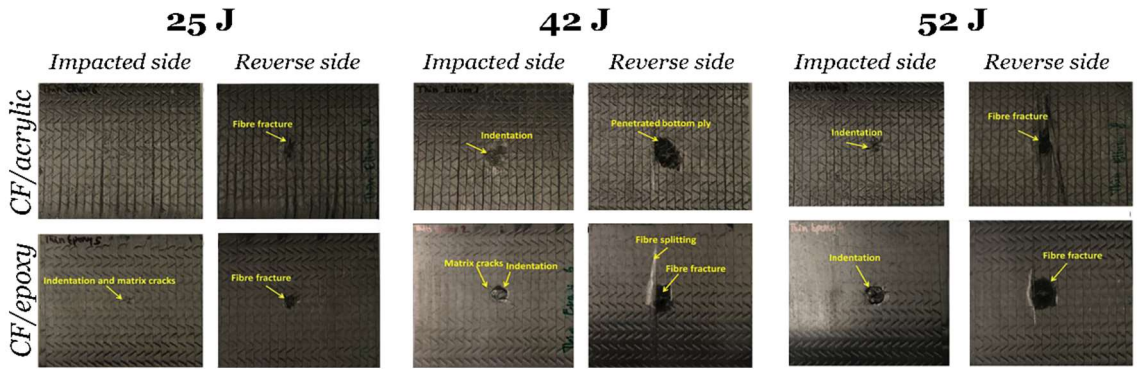

Figure 14. Impact side and reverse side damage following impact events at 25, 42 and 52 J (Copyright permission from Elsevier. Reproduced from Figs. 12, 14 & 16 in [34]).

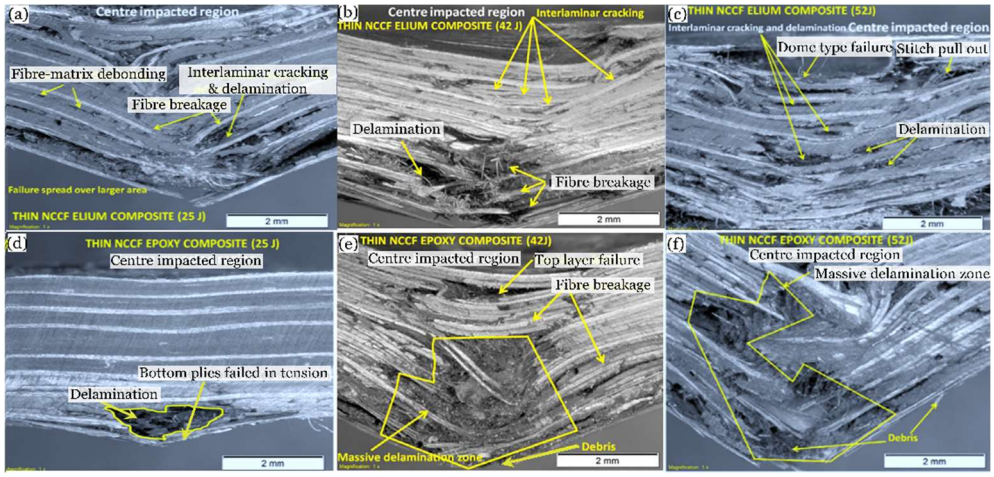

Figure 15. Micrographs showing damage sustained by carbon fibre-reinforced (a), (b) & (c) acrylic and (d), (e) & (f) epoxy composites following drop-weight impacts at 25, 42 and 52 J, respectively (Copyright permission from Elsevier. Reproduced from Figs. 13, 14 & 15 [34]).

4.2.4 Interlaminar fracture toughness

4.2.4.1 Mode-I interlaminar fracture toughness

Quasi-isotropic thin-ply carbon fibre-reinforced acrylic composites have been reported to exhibit superior Mode-I fracture toughness than equivalent epoxy-based composites due to the prevalence of crack arresting mechanisms such as crack deflection behind the crack tip, crack branching and multi-plane propagation of cracks [57]. The authors reported fibre bridging, strong interfacial strength, ductile drawing and crazing, fibre splitting and pull-out for the acrylic-matrix composite material, whereas the epoxy-based composite was reported to exhibit clean fibre failure and pull out, brittle propagation of matrix cracks and scarp formation. Higher peak loads were reported for the acrylic-based samples than their epoxy counterpart, indicating superior resistance to crack initiation. The authors reported a superiority in bond strength and adhesion in both thick- and thin-ply carbon fibre-reinforced acrylic composites relative to the thin-ply epoxy-matrix composite. This work also highlighted the effects of ply thickness on the Mode-I interlaminar fracture toughness, which are believed to have their origins in the size of the interlaminar resin-rich layer thickness. This is supported by the findings reported by Bhudolia et al. [35]. More importantly, these works highlight that even thick-ply acrylic-matrix composite outperforms its thin-ply epoxy counterpart in both initiation and propagation fracture toughness.

4.2.4.2 *Mode-II interlaminar fracture toughness*

Barbosa et al. [58] found that woven carbon fibre-reinforced acrylic exhibited superior Mode-II propagation toughness (+40 %) than its epoxy-matrix counterpart. The load-displacement responses for both materials are presented in Figure 16 (a) and Figure 16 (b).

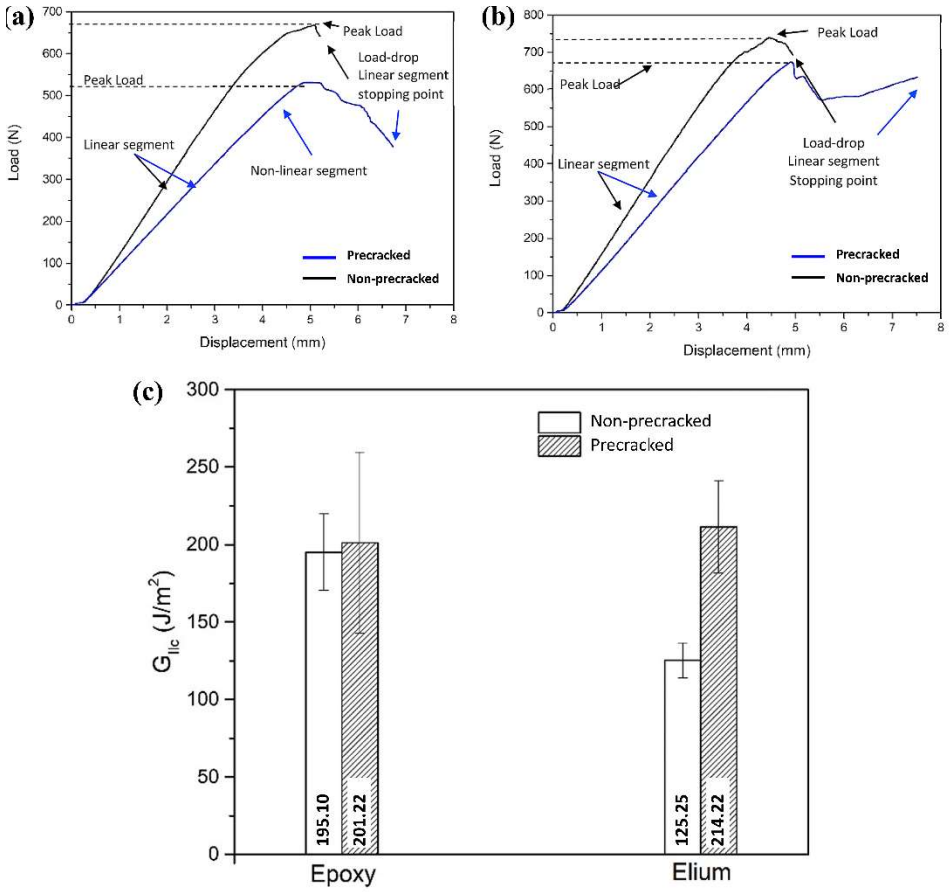

Figure 16. Load-displacement curves for carbon fibre-reinforced (a) E-150, (b) epoxy; and (c) Mode-II interlaminar fracture toughness determined from same (Copyright permission from Elsevier. Reproduced from Figs. 6-8 in [58]).

The authors state that the higher peak load in the epoxy-matrix composite is indicative of superiority in *suppressing* the occurrence of delamination; i.e., a higher energy requirement for initiation. It was also suggested that the superior propagation fracture toughness exhibited by this thermoplastic-matrix composite stems from two mechanisms – plastic matrix deformation and interfacial debonding; which the authors remarked are beneficial in composites subjected to Mode-II loading. In addition to crack propagation, some of the energy absorbed was said to be linked with plastic deformation within matrix-rich zones. This plastic deformation is thought to alter the fracture surface considerably and may mask

important fractographic characteristics. SEM fractographic inspection (Figure 17) revealed characteristic Mode-II fracture behaviour on the surfaces of both materials, namely, shear cusps.

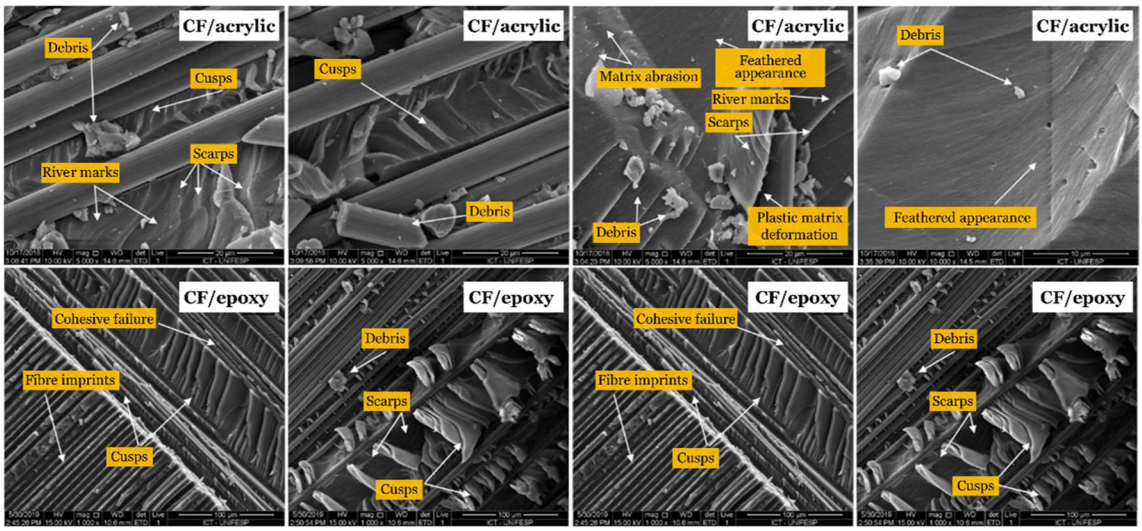

Figure 17. SEM micrographs of Mode-II fracture surfaces of CF/acrylic and CF/epoxy (Copyright permission from Elsevier. Reproduced from Figs. 11 & 12 in [58]).

Cusps are shear-induced fracture features that develop at the interface due to interlaminar shear stresses, which may cause matrix cleavage. They develop in the matrix-rich regions between fibres, following the direction of failure propagation. Micrographs of the fibre surfaces shown in Figure 18 reveal comparable fibre coverage following fracture, indicating that the use of multi-compatible sizing technology may not adversely affect the performance of the acrylic-based system.

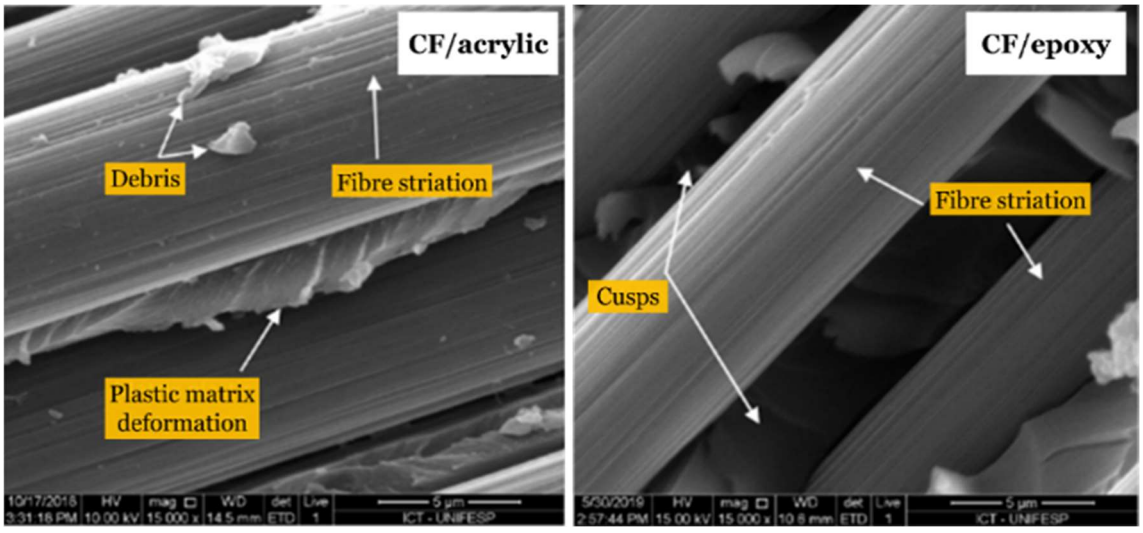

Figure 18. SEM micrographs of exposed fibre surfaces following Mode-II fracture toughness testing on CF/acrylic and CF/epoxy composites (Copyright permission from Elsevier. Reproduced from Figs. 11 & 12 in [58]).

Thus, the variations in G_{IIC} between precracked and non-precracked test configurations may not be linked with variations in interfacial adhesion. The authors did, however, remark that even further enhancements may be realised in the crack resistance of the acrylic-based composites by using specially sized fabrics compatible with acrylic resin systems.

4.3 Flax fibre-reinforced acrylic-matrix composites

4.3.1 Tensile properties

Baley et al. [41] conducted a parametric study to assess the longitudinal tensile behaviour of flax fibre-reinforced acrylic composites alongside polyamide-, polypropylene-, and epoxy-based counterparts. For the purpose of this review, the measurements reported by the authors have been normalised to equivalent fibre volume fractions of 50 %. Although matrix type yielded marginal effects on the tensile moduli across all samples, the most significant influence was observed in strengths. The acrylic-matrix composite was found to be superior in tensile strength to the flax fibre-reinforced polypropylene (+23 %) and maleic anhydride-grafted polypropylene (+7 %). However, its tensile strength was 58 % lower than the epoxy-based laminate and comparable to the polyamide-based material. Chilali et al. [45] also studied the static tensile behaviour of woven flax fibre-reinforced epoxy and acrylic laminates alongside their unreinforced forms. The authors observed ductile and quasi-linear behaviour in the unreinforced acrylic and epoxy matrices, with failure strains of 2.3 % and 1.1 %, respectively. For reinforced composites, three distinct stress-strain characteristic regions were identified. Both the acrylic- and epoxy-based materials were reported to exhibit an initial linear elastic region. This region was preceded by a region of slight non-linearity, with a loss of stiffness being reported. Lastly, stress increases linearly up to ultimate failure, with both materials failing abruptly thereafter. This variation has also been reported in other works by Haggui et al. [59,60], who describe the same trend in stress-strain response for unidirectional flax fibre-reinforced acrylics. All authors attribute the second stage (non-linear) with the creation and evolution of damage. However, the authors present different explanations for the third and final stage. Haggui et al. [59,60] suggest that this quasi-linear behaviour is associated with multiplication or intensification of damage,

leading up to ultimate failure, whereas, Chilali et al. [45] proposed contributions from microfibrillar reorientation associated with flax fibres. As shown in

Table 4, the tensile properties reported by Chilali et al. [45] appear to be significantly lower than those reported by other authors. However, this may be due to the differences in reinforcement architecture used and the high variability of flax fibres being natural fibres [61].

Table 4. Summary of tensile properties reported for flax fibre-reinforced acrylic composites.

	V_f	V_f*	σ (MPa)	σ** (MPa)	E (GPa)	E** (GPa)
Baley et al. [41]	48	50	243.8	**254.0**	27.6	**28.8**
Chilali et al. [45]	37.1	50	130	**175.2**	13.53	**18.2**
Haggui et al. [59,60]	38	50	210	**276.3**	23	**30.3**
Monti et al. [107]	~37.5	50	225	**300**	23.3	**31.1**

All data has been normalised to a target V_f (marked *) of 50 % for the purpose of this review.
Reported data and normalised data (marked **) have been presented.

4.3.2 Compressive properties

Baley et al. [41] presented findings of a study on the comparative compressive performance of unidirectional flax fibre-reinforced acrylic and epoxy composites. The authors reported 7%, 27% and 5% lower compressive strength in the acrylic-based material than its epoxy (115 MPa), polyamide (134 MPa), and polypropylene/maleic anhydride-grafted polypropylene (110 MPa) counterparts, respectively. However, it had 28 % higher compressive strength than flax fibre-reinforced polypropylene (75 MPa). In terms of tensile strength, it was superior to the flax fibre-reinforced polypropylene (193 MPa; +23 %) and maleic anhydride-grafted polypropylene (234 MPa; +7 %). However, its tensile strength was 58 % lower than the epoxy-based laminate (408 MPa) and comparable to the polyamide-based material (258 MPa). These results clearly show a more considerable influence of the matrix used on compressive strength than on tensile strength, a property known to be fibre-dominated. The authors attribute the poor compressive performance of the acrylic to weak interfacial strength between the flax fibres and acrylic matrix. These

results clearly show a considerable influence of the matrix used on compressive strength, which itself is known to be matrix-dominated.

4.3.3 Flexural properties

Haggui et al. [59] evaluated the flexural behaviour of bidirectional flax fibre-reinforced acrylic laminates using three-point bend tests. A three-stage stress-strain behaviour was described, with an initial linear region preceding a nonlinear and terminal quasi-linear one. The authors also reported transverse microcracking as the incipient damage mechanism, occurring during the nonlinear phase of testing. Haggui et al. [59] studied the cyclic flexural performance of flax fibre-reinforced acrylics and identified a two-stage degradation of stiffness. The authors concluded that a critical number of cycles (c. 10^4) exists, below which the rate of degradation is relatively slow. This was believed to be related to damage initiation and microcracking phenomena, which precede the rapid accumulation of transverse cracking and subsequent delamination growth up to 9×10^5 cycles.

4.3.4 Shear properties

Chilali et al. [45] assessed the shear performance of flax fibre-reinforced acrylic and epoxy laminates by in-plane shear testing and reported a superiority (~10 %) in shear modulus for the epoxy-based material. Both flax fibre-reinforced acrylic and epoxy materials were reported to exhibit equivalent ultimate shear strengths at approximately 23 GPa; however, normalising the reported data revealed an even greater difference in the measured values. The epoxy-based laminate possessed higher (+16 %) shear strength than the acrylic material.

4.4 Dynamic mechanical (thermomechanical) properties

Several works have studied the thermomechanical behaviour of thermoplastic acrylic matrices and their glass fibre-reinforced composites. Acrylic-based composites have been reported to exhibit comparable (and in some case, superior) performance to their thermosetting counterparts, such as epoxy-matrix composites with T_g values in the range of 67°C - 127 °C being reported [25,37,47,51,62–65]. Table 5 presents a summary of some of the key reported thermomechanical properties of acrylic matrix composites in published literature.

Table 5. Summary of some thermomechanical properties reported in published works for acrylic-based matrices and composites.

Materials	*Results*	*References*
Matrix: E-180, E-188 Reinforcement: UD Glass NCF Sizing: Multi-compatible	i. T_g: 115 °C Tan delta peak: 0.53	[51]
	ii. T_g: 106 °C Tan delta peak: 0.76	[37]
Matrix: *(E-X) Grade not specified* Reinforcement: *Not specified* Sizing: *Not specified*	i. T_g: 125 °C Tan delta peak: -	[65]
	ii. T_g: 127°C Tan delta peak: -	[64]
Matrix: E-150† Reinforcement: *Not specified* Sizing: *Not specified* †Various initiator contents: 0.8-1.6 wt. %	T_g: 116° C, 123° C, 123 °C Tan delta peak: ~0.5, ~0.45, ~0.65 *0.8 wt. %, 1.2 wt. % and 1.6 wt. %, respectively*	[25]
Matrix: E-C595E Reinforcement: *Not specified* Sizing: *Not specified*	T_g: 109 °C *As produced* T_g: 119 °C	[47]
Matrix: E-C595E Reinforcement: UD Glass Sizing: contains a vinyl group	*Processed at 190°C; 10 min* T_g: 122 °C	
Matrix: E-150 Reinforcement: - Sizing: *Not specified*	T_g: 110 - 120°C Tan delta peak: 1.3 (matrix only)	[63]
Reinforcement: Carbon fabric* (thin- and thick-ply) Sizing: *Not specified* *quasi-isotropic lay-up	Tan delta peak: 0.59 (thin-ply) Tan delta peak: 0.51 (thick-ply	

4.5 The effects of fibre sizing on the properties of acrylic-matrix composites

Given the infancy of this class of resins, its chemistry is not as well-known as that of traditional thermosets, which are associated with well-established supply chains and dedicated sizing technology. Until recently, much of the published literature on acrylic-matrix composites comprised fibre reinforcements with multi-compatible sizing. With advancing research, there are now specially sized reinforcement systems available for acrylic matrix composites. However, being based on novel technology, these systems require comprehensive characterisation. Several authors have investigated the effects of such acrylic-sized reinforcements against their multi-compatible counterparts. The following section summarises the findings to date.

Boufaida et al. [40] studied the influence of sizing on the properties of glass fibre-reinforced acrylic composites using fibres sized with multi-compatible (MC) and acrylic-compatible (AC) formulations. Fibre-matrix strength was assessed in the materials using monotonic and fatigue in-plane shear testing. Although no notable influences were reported on modulus and strength, the authors reported a lower threshold for the development of progressive damage in MC-sized samples in response to monotonic loading, with an enhancement of only 4 % in strength reported for the use of AC sizing. On the influence of sizing on fatigue damage development, damage-induced heat build-up was reported for both materials alongside a reference with no sizing (NS). It was found that the use of MC-sized fabrics results in enhanced fatigue performance (+7 % compared to the NS reference). However, a more significant difference was reported for the AC-sized material, corresponding to a 22 % improvement with respect to the NS reference. Although this study evaluated macromechanical performance, their findings were in agreement with those of Beguinel et al. [66], who studied the effects of fibre sizing on the interfacial shear strength (IFSS) of glass fibres with acrylic-compatible and polypropylene-compatible sizings, and carbon fibres with acrylic-compatible- and epoxy-sizings. Microbond test samples were prepared using a reactive acrylic matrix on single tensioned fibres. Improved IFSS values were reported for glass- and carbon-reinforced acrylic samples comprising fibres with acrylic-compatible sizing (compared to those employing multi-compatible sizing formulations). Interestingly, Davies et al. [67] suggest that the use of appropriate sizings may affect the durability of glass fibre-reinforced acrylic composites.

Shanmugam et al. [68] demonstrated fibre surface functionalisation of ultra-high molecular weight polyethylene (UHMWPE) as a viable means of improving Mode-I interlaminar fracture toughness. The authors studied the effect of treating fibres with two polydopamine (PDA)-based coatings for composite applications. As evident in Figure 19, the effects of these treatments on fracture behaviour were significant. Comparing the fracture behaviour of the FRP (Figure 19a and Figure 19b) with untreated fibre to that containing PDA-treated fibres (Figure 19c and Figure 19d), the authors reported smooth fibre surfaces with the use of untreated fibres and the presence of residue on treated fibre.

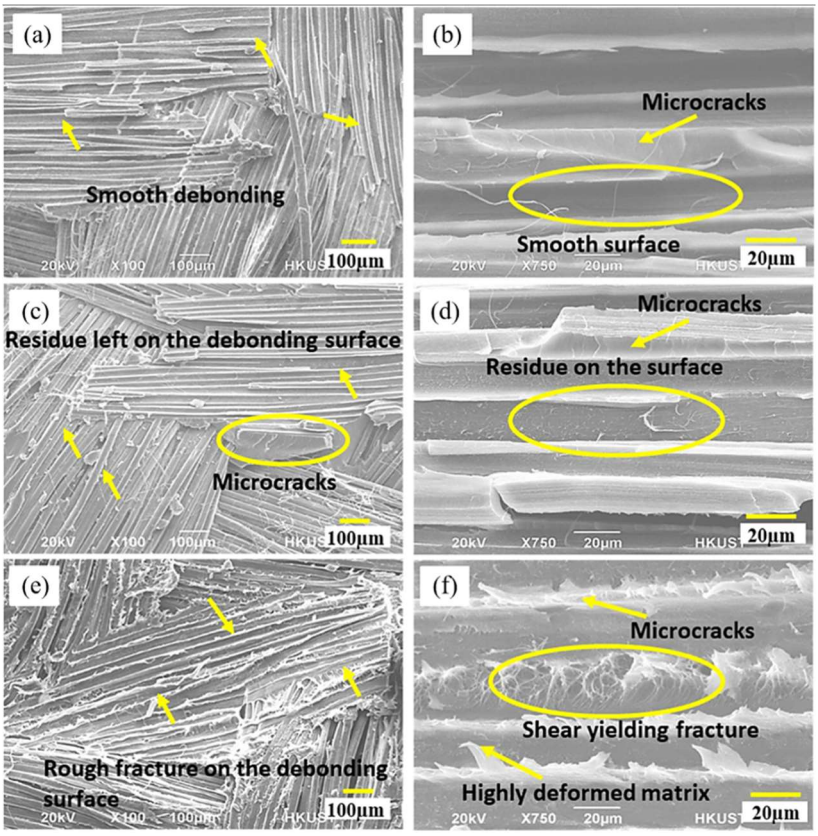

Figure 19. Low- and high-magnification SEM micrographs of double cantilever fracture surfaces of UHMWPE-acrylic samples containing (a & b) untreated fibres, (c & d) PDA-treated fibres, and (e & f) PDA+MWCNT-treated fibres (Copyright permission from Elsevier. Adapted from Fig. 7 in [68]).

Thus, it was evident that fibre functionalisation with PDA alone resulted in enhanced interfacial adhesion with the E-188 matrix used, corresponding to 19.6 % improvement in average fracture toughness. Furthermore, the enhancements achieved with the sample shown in Figure 19e and Figure 19f were realised with the incorporation of 0.03 wt. % of multi-walled carbon nanotubes (MWCNT) into the PDA coating.

For this sample, an improvement of 42.5 % in fracture toughness was reported against its untreated counterpart.

These works highlight the requirement of specialised sizing technologies for these acrylic resins; however, several authors [28,37,38,51,69] have shown that the use of MC-sized reinforcement does not result in any adverse effects on the quality and performance of the composites. Interestingly, these authors report the use of E-180 or 188 resins with MC-sized glass fibre reinforcement. These studies may highlight the suitability of the Elium® 18* family of resins for use with existing glass fibre sizing technologies. Besides, in a study by Charlier et al. [69], the IFSS of an unspecified Elium® resin with MC-sized and AC-sized glass fibres were micromechanically assessed by fragmentation and microdroplet testing. No significant improvements in IFSS were reported with the use of specialised sizings for acrylic matrices on glass fibres. These findings constitute important knowledge, given that the use of appropriate glass fibre sizing technology is a prerequisite for effective interfacial stress transfer, desirable fibre strength and the ultimate resistance to aggressive physical, chemical and environmental degradation agents [70].

4.6 Toughening of acrylic-matrix composites

Matrix toughness is known to contribute significantly to the behaviour of a laminate, particularly its interlaminar fracture behaviour [64], which affects damage tolerance [65]. Thermoplastic matrices are naturally superior in toughness to their thermosetting counterparts and as such, typically exhibit higher Mode-I interlaminar fracture toughness and other matrix-dominated characteristics. However, in these works [34,35,57], acrylic-based composites were only marginally higher in Mode-I interlaminar fracture toughness than their epoxy-based counterparts – highlighting a requirement for the development of appropriate toughening strategies. To date, the intrinsic toughness of traditional high-performance thermoplastic matrices obviates the requirement for toughening; as such, the effects of a strategically developed approach for acrylic-based composites need to be understood.

The influence of toughening on unreinforced and reinforced acrylic matrices have been investigated in several works [32,52,64,65,71,72]. All studies focused on benchmarking a toughened acrylic matrix – Elium Impact® alongside an untoughened grade. This modified grade reportedly contains 10 wt. % of a self-assembling acrylic block copolymer additive, Nanostrength®. However, the base grade of Elium®

within the so-called Elium Impact® is not specified in any of the cited works. Nanostrength® is based on Arkema's proprietary alcoxyamine technology, comprising polymethylmethacrylate-b-polybutylacrylate-b-polymethylmethacrylate (shown in Figure 20).

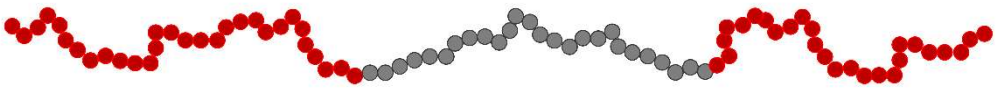

poly[(methyl)methacrylate]-b- poly(butyl acrylate)-b-poly[(methyl)methacrylate]

Figure 20. Structure of self-assembling acrylic block copolymer (Copyright permission from Elsevier. Reproduced from Fig. 1a in [32]).

In addition to Nanostrength®, acrylonitrile butadiene styrene (ABS) has also been applied as a toughening agent [52]. Like Nanostrength®, ABS is a block copolymer but contains a uniformly dispersed phase of rubber within a styrene-acrylonitrile matrix. The effects of the incorporation of these toughening agents on the performance of acrylic-matrix composites will be discussed herein. Table 6 presents an overview of published works in this area.

The use of Nanostrength® within a glass fibre-reinforced acrylic hybrid laminate has been shown to reduce the energy absorbed for damage development when compared to the equivalent untoughened laminate [32]. Similarly, Kinvi-Dossou et al. [52] reported enhanced impact strength in Nanostrength®-toughened acrylic, both in unreinforced and glass fibre-reinforced forms, as detailed in Table 6. However, ABS-toughening proved more effective at enhancing polymer and composite impact strengths than the use of Nanostrength®. In the same work, the authors also studied drop-weight impact performance of the same materials; however, impacts under 40 J did not appear to be influenced by toughening. Both tougheners contain rubber nanophases, which become grafted to the matrix during the *in situ* polymerisation process, rendering it more ductile. This enhanced ductility facilitates plastic deformation within the matrix in response to low-velocity impacts. In the case of Nanostrength®, it is believed to play a vital role in crack bridging and suppressing coalescence of voids and microcracks. The authors also suggest that the self-assembling ability of Nanostrength® is essential to the micelle cavitation mechanism, which not only toughens the matrix but induces shear banding and resists the initiation of delamination. These conclusions are in agreement with those drawn by Boumbimba et al. [32]. They are further supported by the works of Pini et al. [65,72,73],

who extensively studied the fracture behaviour of untoughened and toughened acrylic matrix systems and identified the dominant roles played by crazing, cavitation and shearing in Nanostrength®-toughened acrylic matrices. Pini et al. [65] suggested a transition from crazing to cavitation and shearing depending on temperature and strain-rate conditions and reported differences in the respective dependences of Mode-I fracture toughness on crack propagation rates for the toughened and untoughened acrylic-matrix

Table 6. Overview of works on the effects of toughening on the impact performance of acrylic-matrix composites.

Materials	*Summary of results*	*Comments*	*Ref.*
E-150 Nanostrength® (5–15 wt. %) Glass fibre (woven) Drop-weight impact	• Enhanced impact damage resistance (20°C and 80°C impacts only). Increase in matrix ductility and reduced damage extension with Nanostrength® toughening. • 10 wt. % loading conferred superior performance in most cases as shown by changes in absorbed energy relative to the unmodified material: ▪ *-80°C impacts* → -4 % (30 J); -35 % (40 J); -13 % (50 J) ▪ *20°C impacts* → -31 % (30 J); -5 % (40 J); +7 % (50 J) ▪ *80°C impacts* → -6 % (30 J); -17 % (40 J); -10 % (50 J) • Proposed toughening mechanisms: crack-bridging, micelle cavitation, shear banding and crack tip shielding.	Explored a breadth of variables, which are insightful for the composites community in terms of the impact behaviour of toughened acrylic-matrix composites. However, the effects of individual variables was not readily understood. Moreover, no quantitative damage zone assessments were performed.	[32]
E-150 ABS (10 wt. %) Nanostrength® (10 wt. %) Glass fibre Drop-weight impact & Charpy impact	• Nanostrength® and ABS toughening of acrylic polymer and composite only moderately enhanced the absorbed energy in toughened laminates for drop-weight impact: ▪ *ABS-toughened acrylic* →-19 % (40 J); -0 % (50 J); -7 % (60 J) ▪ *Nanostrength®-toughened acrylic* →-16 % (40 J); +8 % (50 J); -2 % (60 J) • Significant improvements in Charpy impact resistance unreinforced samples: ▪ *ABS-toughened acrylic* →+238 % (unreinforced polymer) ▪ *Nanostrength®-toughened acrylic* →+43 % (unreinforced polymerProposed toughening mechanisms for Nanostrength® and ABS: crack-bridging, void coalescence, micelle cavitation, shear banding and crack tip shielding.	Findings are logically presented and discussed with the effects of toughening, reinforcements and energy levels considered. However, no quantitative damage zone assessments were performed.	[52]

composites. The fracture toughness of the toughened-matrix composite exhibited inverse proportionality to strain-rate; as the crack propagation rate increased, the authors reported a decreasing trend in fracture toughness. Interestingly, no rate effects were reported for the unmodified-matrix composite. These observations are further explained in work by Pini [53], which showed that higher displacement rates (and lower temperatures) promote multiple crazing in the Nanostrength®-toughened acrylic matrix. Conversely, cavitation and shear yielding are the dominant mechanisms at lower displacement rates (and higher temperatures). The rubber particles within the toughened acrylic matrix are said to both initiate and control the crazing behaviour. While a few larger crazes were reported for unmodified acrylic matrix, toughening was said to give rise to the formation of a large number of smaller crazes; the relative increase in the volume saturated by these smaller crazes is believed to contribute to favourable energy absorption within the toughened matrix. Cavitation in the vicinity of rubber particles was said to promote matrix plasticity as opposed to being a primary energy absorption mechanism. Another role of cavitation in the toughened matrix is to shear yielding, which like crazing, constitutes a major energy absorption mechanism.

Pini [53] also reported positive effects of toughening on the interfacial adhesion; unmodified acrylic-matrix composites exhibited inferior interfacial strength to the toughened composites, which showed evidence of cohesive fracture of the fibre-matrix interface. However, fibre bridging was more prevalent in the unmodified composite during testing. Finally, the author reported more effective toughness transfer from unreinforced matrix to reinforced composite in the case of the unmodified matrix for which full transfer was reported due to the absence of interactions between the fibres and the process zone in the matrix-rich layer. This was not the case for the toughened materials, where only a partial transfer was reported. The author attributes this to contributions from fibre-process zone interactions. A smaller process zone (as in the untoughened matrix) was thought to be constrained by adjacent fibres. As the size of the process zone increases (with the incorporation of a toughening phase), its development is thought to be more affected by the presence of the fibres. Furthermore, the crack tip opening distance and thickness of the interlaminar resin-rich layer were shown to be influenced by the presence of a toughening phase within the matrix. Pini cites rheological differences in the toughened and untoughened material as the source of these observed differences.

In general, rubber toughening of polymeric materials is known to compromise their mechanical [74,75] and thermomechanical performance by decreasing T_g [76]. Owing to their non-reactive backbone, block copolymers like Nanostrength® are said to be unique, in that their use reportedly yields no reduction in T_g [77]. To date, mechanical and thermomechanical characterisation of Nanostrength®-toughened acrylic matrices and their composites remain mostly unexplored. However, the work of Pini [53] provides valuable insights into the fracture behaviour. The author reported a deleterious effect of Nanostrength®-toughening on matrix stiffness due to the presence of the rubber phase. The authors reported enhancements in tensile failure strains at a constant displacement rate of 1 mm/min over a range of test temperatures (0-60°C). Unmodified acrylic matrix (grade unspecified) exhibited brittle failure characteristics with strains of ~0.025-0.2, whereas the incorporation of 10 wt. % of Nanostrength into the same matrix system produced more ductile failure with strains of ~0.2-0.9. Table 7 presents a summary of key published works on the thermomechanical performance of Nanostrength®-toughened acrylic (Elium Impact®). Due to the paucity of works on the thermomechanical properties of toughened acrylic-matrix composites, only findings on toughened unreinforced acrylic polymer have been presented in Table 7.

Table 7. A summary of the effects of Nanostrength®-toughening on glass transition temperatures of unreinforced acrylic polymers.

Matrix	*Glass transition temperature (°C)*	*Reference*
Elium®	125	Pini et al. [65]
	127	Pini et al. [64]
Elium Impact®	-25, 125	Pini et al. [65]
	-25, 130	Pini et al. [64]

5 Advantages of thermoplastic acrylic-matrix composites

5.1 Reshaping by thermoforming

Cousins et al. [22,46] successfully demonstrated the thermoformability of continuous fibre-reinforced acrylic composites. An acrylic-matrix prototype spar cap section was flattened (120°C, 5.4 kPa, 8 h; radio-frequency press) as shown in Figure 21a, and a prototype single-curvature component (Figure 21 b) was also produced as part of this study. Such works are essential to the cross-sectoral appeal; particularly for the automotive industry, where *in situ* polymerised blanks could be readily thermoformed, facilitating mass-

production. However, further investigation would be essential to understanding the effects of thermal reprocessing on matrix, fibre and interfacial properties.

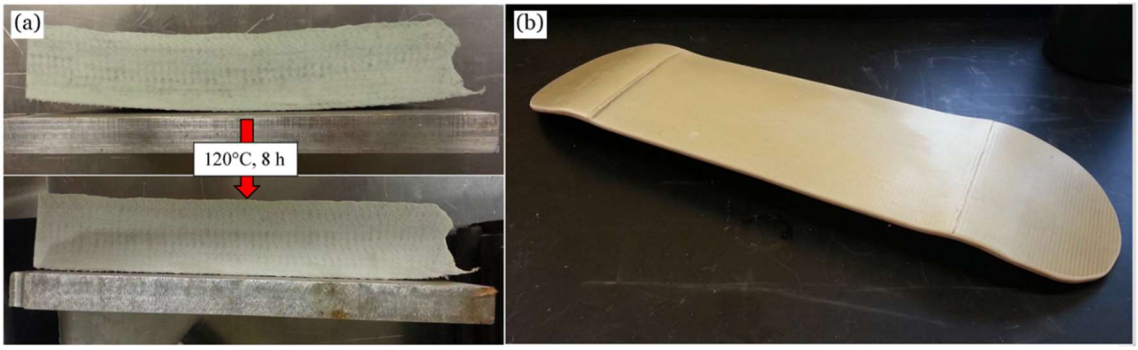

Figure 21. Demonstration of thermoformability (a) flattening a curved section and (b) producing a curved prototype from glass-reinforced acrylic laminates (Copyright permission from Elsevier. Reproduced from Fig. 9 & 10 in [22]).

5.2 Joining of acrylic-matrix composites

Welding is an attractive alternative to mechanical fasteners and adhesive joining. The former adds undesired weight and may cause drilling-induced delamination and bearing failure. The bondline achieved with the latter is sensitive to harsh chemical environments, which can compromise static and dynamic structural performance [38]. Some recent works have demonstrated the weldability of glass fibre-reinforced acrylic composites [38,39,78]. Fusion welding of glass fibre-reinforced acrylic substrates to form lap-shear coupons was readily realised above 110°C (T_g of E-188) using several element types (fine stainless steel mesh, woven carbon and unidirectional carbon fabrics) [38]. Bhudolia et al. [39] comparatively assessed ultrasonically welded and adhesively bonded carbon fibre-reinforced acrylic joints based on E-150. The authors reported the use of an integrated semi-hemispherical energy director design for some of the welded joints and Arkema's methacrylate-based adhesive system (Bostik SAF 30 5) for the adhesively bonded reference coupons. The joint configurations used for welded samples are schematically represented in Figure 22 with the volume of neat resin used in forming the energy director within the joints.

Configuration		Resin Volume (mm^3)
ELC_IED		150.7
ELC_FED (0.5mm ELF)		312.5

Figure 22. Welding configuration used by Bhudolia et al. [39] (Copyright permission from Elsevier. Fig. 1 in [39]).

Energy directors have also been shown by Bhudolia et al. [39,78] to cut down on joining time compared to adhesive bonding by 99.8 %. Additionally, Bhudolia et al. [39] reported 23 % higher static lap shear strengths and 12 % higher fatigue strengths in welded joints compared to their adhesively bonded counterparts. The authors observed fibre impingement and shear cusps as the primary failure mechanisms, concluding that these promoted strong interfacial adhesion. Murray et al. [38] reported up to 100 % higher static lap shear strengths in resistance and induction welded coupons relative to the adhesively bonded variants. It was also suggested even greater potential enhancements of joint performance may be realised using fibre-reinforced heating elements with improved sizing technology and infusion quality.

5.3 Recycling and recovery of constituents

Cousins et al. [22] demonstrated the viability of acrylic-matrix composites for recycling by conventional recovery methodologies employed today such as pyrolysis, mechanical grinding and dissolution. The authors compared the recoverable constituents as well as the energy and cost requirements for all techniques, concluding that dissolution was the most favourable approach based on full-scale fibre and polymer recovery as shown in Figure 23. Compared to virgin fibres, recovered fibres were reported to exhibit no loss in tensile strength, with a 12 % reduction in stiffness. This loss in stiffness was attributed to operator-induced fibre misalignments during the dissolution recovery process. Additionally, pyrolysis was reported to result in the loss of fibre length scale and sizing; dissolution facilitated not only their retention but also the recovery of the acrylic polymer.

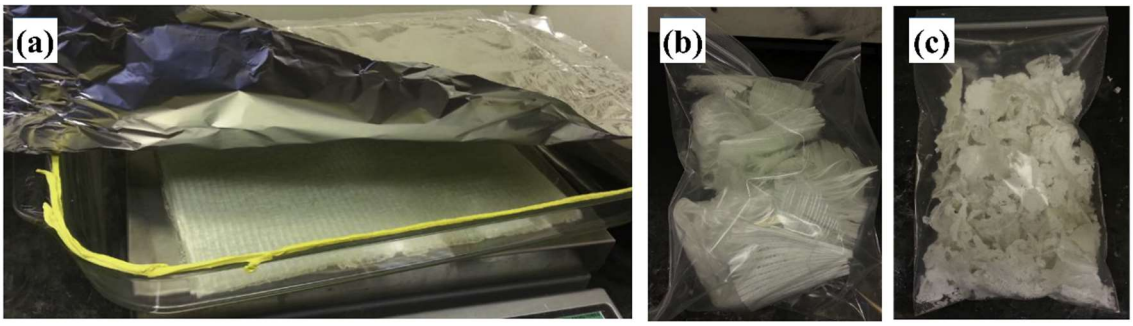

Figure 23: Recovery of fibres and polymer matrix from *in situ* polymerised glass/acrylic laminate by dissolution as demonstrated by Cousins et al. [22] (Copyright permission from Elsevier. Reproduced from Fig. 5 in [22]).

Pyrolysis was deemed less viable for the acrylic-matrix composite, as this required 78 % more decomposition energy than the requirement for the epoxy-based reference. Grinding and dissolution consumed the lowest and highest energy, respectively, per unit of mass. The works of these authors essentially answer the questions raised by Baley et al. [41] on the recyclability of these novel acrylic-matrix composites. Although the findings reported by Cousins et al. [22] suggest no loss of sizing using the dissolution approach, surface analyses could substantiate this conclusion and contribute to increased confidence in these materials as potential future-proof solutions in terms of overall end-of-life value. Dissolution in acetone has also been demonstrated as a potential route to material recovery [79].

One of the challenges associated with composites recycling is that recovery methodologies only facilitate down-cycling, with low-level application of the recyclates due to process-related loss of structural integrity. The attainment of higher levels in the recycling hierarchy is therefore, more crucial than ever to realise true circularity in this market [80]. Ultimately, processes like pyrolysis and dissolution offer better prospects in terms of fibre length-maintenance; however, dissolution affords even greater benefits in terms of polymer matrix recovery [22]. In particular, the potential for selective dissolution combined with the reshapability of continuous fibre-reinforced acrylic composites as discussed in Section 5.1 could be attractive. The property-retention facilitated by dissolution recycling processes may enable the exploration of high-value recycling and reuse of end-of-life acrylic-matrix composites.

These works go a long way to answering important research questions, which have profound ecological implications. Full or partial recovery of resources from end-of-life components manufactured from acrylic-matrix composites can mean better end-of-life waste management. In terms of tonnage, retired thermoset-

matrix composite blades account for a large percentage of landfill-bound waste. It is said that current practices in the marine sector mean that all end-of-life composite waste is typically disposed of in landfill due to contamination with oils, paints and core materials [81]. Given the energy-intensive production methods involved in the fabrication of such components, the use of thermoplastic-based composites has not only been identified as a viable solution to minimising environmental impact, but also potentially has far-reaching economic implications [22].

6 Hybrid thermoplastic composites using *in situ* polymerised acrylics

Matrix- and fibre-based hybridisation have been shown as viable means of providing essential performance enhancements, while concurrently targeting the reduction of mass and overall costs [82,83]. Recent advancements in liquid acrylic-matrix hybrid composites are discussed herein.

Kazemi et al. [84] reported improvements of up to 150 % in the compressive strength of woven carbon fibre/ultra-high molecular weight polyethylene (UHMWPE) fibre-reinforced acrylic hybrid composite systems, with respect to UHMWPE-only fibre-reinforced acrylic reference laminates. Unsurprisingly, this corresponded to 27 % lower strengths in the hybrids, relative to the carbon fibre-reinforced acrylic reference laminate, due to the superiority of carbon fibres in performance. While studies of this type play vital roles in improving our understanding of carbon and UHMWPE as reinforcements in acrylic-matrix hybrid composites, the authors fail to provide comprehensive conclusions of their findings. No remark was made on the implication of such hybrids. Nonetheless, this study does demonstrate the potential for realising more economical (compared to carbon-only FRPs), stronger and stiffer (compared to UHMWPE-only FRPs) thermoplastic hybrid systems by a conventional room-temperature vacuum infusion process. In another study by Kazemi et al. [85], similar hybrids were shown to enhance impact performance, evidenced by a lesser (-47 %) reduction in structural integrity and 18 % reduction in absorbed energy.

Fibre-metal laminates (FMLs) are a class of hybrids comprising thin metal sheets interleaving FRP layers. They were developed to exploit the weight-saving benefits of composites in a relatively cost-effective manner with possible enhancements in fire resistance, damage tolerance, fatigue and impact properties [86,87]. Some of the earliest works in this area focused on the use of thermosetting matrices with glass-reinforced epoxies. This was due to the historic challenges associated with melt processing methodologies

for thermoplastic alternatives. The rise in the popularity of liquid reactive thermoplastic resins has opened doors of opportunity for this class of hybrids, as they facilitate resin infusion processing of thermoplastic FMLs. An overview of works in this area, demonstrating the suitability of liquid thermoplastic acrylic resins is presented in Table 10. While Mamalis et al. [88] relied on drilled holes for through-thickness resin flow during vacuum infusion processing (Figure 25), Shanmugam et al. [89] did not report similar measures to enhance flow. Additionally, it is worth pointing out that although the Mode-I interlaminar fracture toughness reported by Mamalis et al. [88] was lower than the reference acrylic-based laminate, the authors remarked that the value reported for the FML was ~237 % higher than values reported in literature for a thermoset FML.

Table 8. Aluminium alloy surface treatment study parameters as reported for acrylic-based fibre-metal laminates by Mamalis et al. [88] (Copyright permission from Elsevier. From Table 2 in [88]).

Time (min)	Treatment					
	NaOH 10 wt%	Acid solution (ANPE 80/5/5/10)	NaOH 10 wt% + acid solution	Acid solution + NaOH 10 wt%	Sulphuric acid anodising	Atmospheric plasma treatment
2	–	✓	–	–	Def Stan 2003–25/4	1 scan at 1 mm/s
5	✓	✓	✓	✓		1 scan at 2 mm/s
10	✓	✓	✓	✓		3 scans at 1 mm/s
20	✓	✓	✓	✓		3 scans at 2 mm/s

Table 9. Summary of the metal and fibre surface treatments used in acrylic-based fibre-metal laminates by Shanmugam et al. [89].

Laminate	Titanium treatment condition	Fibre surface coating
1. Ti-Pris+UHWPE-Pris	Untreated	No coating
2. Ti-Ann+UHWPE-Pris	Treated	No coating
3. Ti-Ann+UHWPE-PDA	Treated	PDA
4. Ti-Ann+UHWPE-PDA+CNT	Treated	PDA + CNT

Table 10. Overview of some published works on acrylic-matrix hybrid composites.

Materials	*Fabrication Methodology*	*Summary of results*	*Ref.*

• E-188
• BPO
• UHMWPE (woven; 12 plies)
• Ti6Al4V titanium (1.5-mm thick)
• PDA
• CNT (multi-walled)
	A multi-stage process was employed as illustrated in Figure 27b and detailed in Table 9:
	• Alloy surface activation → anodisation, alkali etching and annealing of the alloy sheet.
	• Fibre surface functionalisation → PDA or PDA & CNT fibre coating.
	  • Laminate 1 → Untreated
	  • Laminate 2 → Only alloy surface activation
	  • Laminate 3 → Alloy surface activation + PDA fibre treatment;
	  • Laminate 4 → Alloy surface activation + PDA & CNT fibre treatment.
		• Mode-I fracture toughness improvements relative to the untreated reference laminate (Laminate 1) as shown in Figure 28b:
		  • Laminate 2 → +528 %;
		  • Laminate 3 → +636 %;
		  • Laminate 4 → +916 %.
		• The most significant improvements in crack growth resistance were exhibited by Laminate 4 as evidenced in Figure 28a, Figure 28c & Figure 28d. Failure mechanisms are shown in Figure 28d.
			[89]

• E-180
• BPO
• Glass fabric (UD; 6 plies)
• 6082-T6 aluminium (0.71-mm thick)
• CN104 epoxy acrylate coating
	Multi-stage process the process parameters are summarised in Table 8:
	• Alloy surface activation → chemical etching (alkali, acid, acid-alkali and alkali-acid) or anodisation or atmospheric plasma. The resulting surface morphologies are shown in Figure 24.
	• Alkali-etched aluminium was used in FMLs to promote mechanical interlocking in addition to enhanced chemical adhesion using the CN104 coating.
	  • Laminate 1 → Acrylic-matrix FRP
	  • Laminate 2 → TP-FML
		• Performance of Laminate 2 (relative to the conventional reference laminate (Laminate 1) as shown in Figure 26:
		  • Flexural strength → +10 %;
		  • Flexural modulus → +23 %;
		  • Interlaminar shear strength → +41 %;
		  • Mode-I fracture toughness → -78 %.
			[88]

FML: *fibre-metal laminate;* ***BPO:*** *dibenzoyl peroxide initiator;* ***UHMWPE:*** *ultra-high molecular weight polyethylene;* ***PDA:*** *polydopamine;* ***CNT:*** *carbon nanotubes;* ***UD:*** *unidirectional;* ***FRP:*** *fibre-reinforced polymer;* ***TP-:*** *thermoplastic*

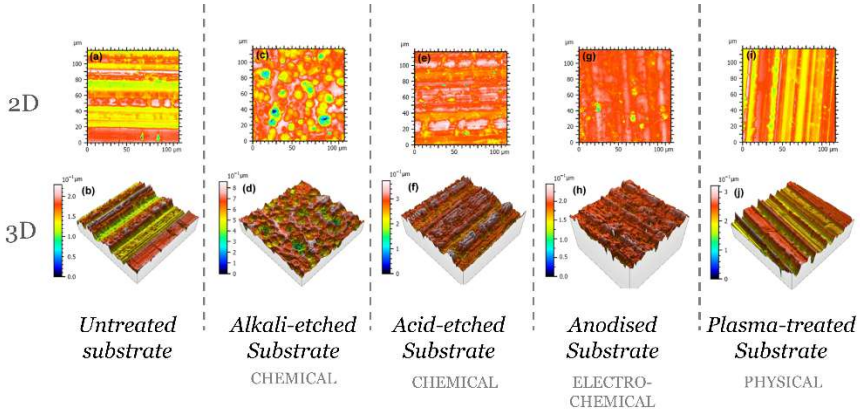

Figure 24. 2D and 3D height profiles for an untreated substrate (a) & (b); and alkali-etched (c) & (d), acid-etched (e) & (f), anodised (g) & (h), and plasma-treated (i) & (j) substrates (Copyright permission from Elsevier. Reproduced from Fig. 2 in [88]).

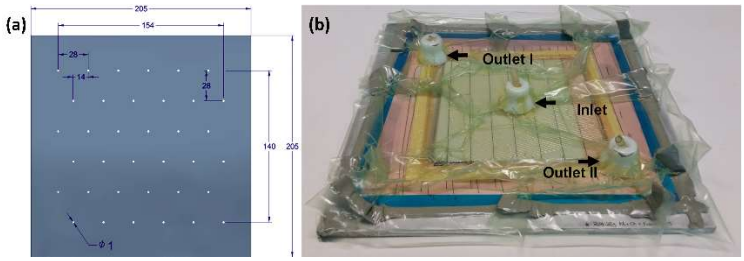

Figure 25. (a) Perforated aluminium sheet (b) Experimental set-up for radial vacuum infusion process as used Mamalis et al. [88] (Copyright permission from Elsevier. Adapted from Fig. 1 in [88]).

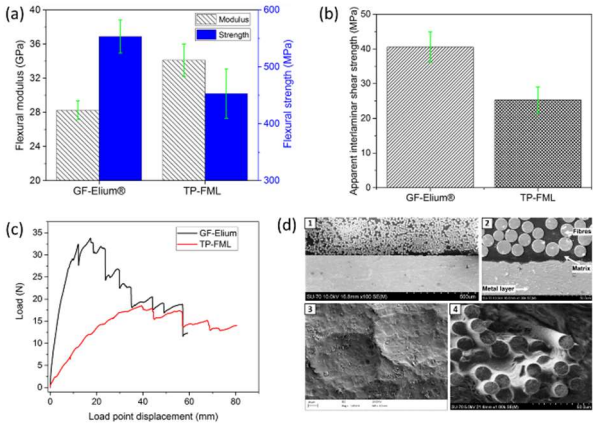

Figure 26. Summary of comparative (a) flexural, (b) interlaminar shear, and (c) Mode-I interlaminar fracture toughness performance of thermoplastic FML and an equivalent FRP reference. (d) Microscopic characteristic of thermoplastic FML studied by Mamalis et al. [88] (Copyright permission from Elsevier. Reproduced from Figs. 5-8 in [88]).

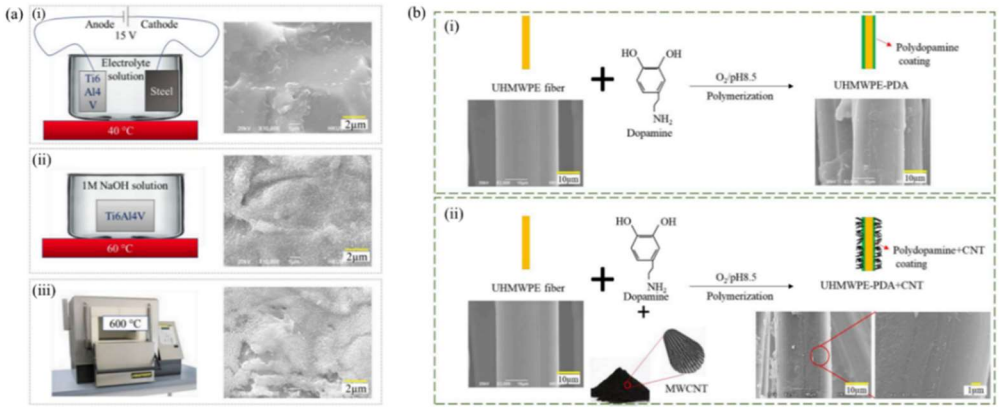

Figure 27. (a) Schematic of the titanium alloy surface treatment sequence; (b) UHMWPE fibre surface treatments using (i) a polydopamine coating only and (ii) a polydopamine coating-impregnated carbon nanotube coating (Copyright permission from Elsevier. Reproduced from Figs. 1 &2 in [89]).

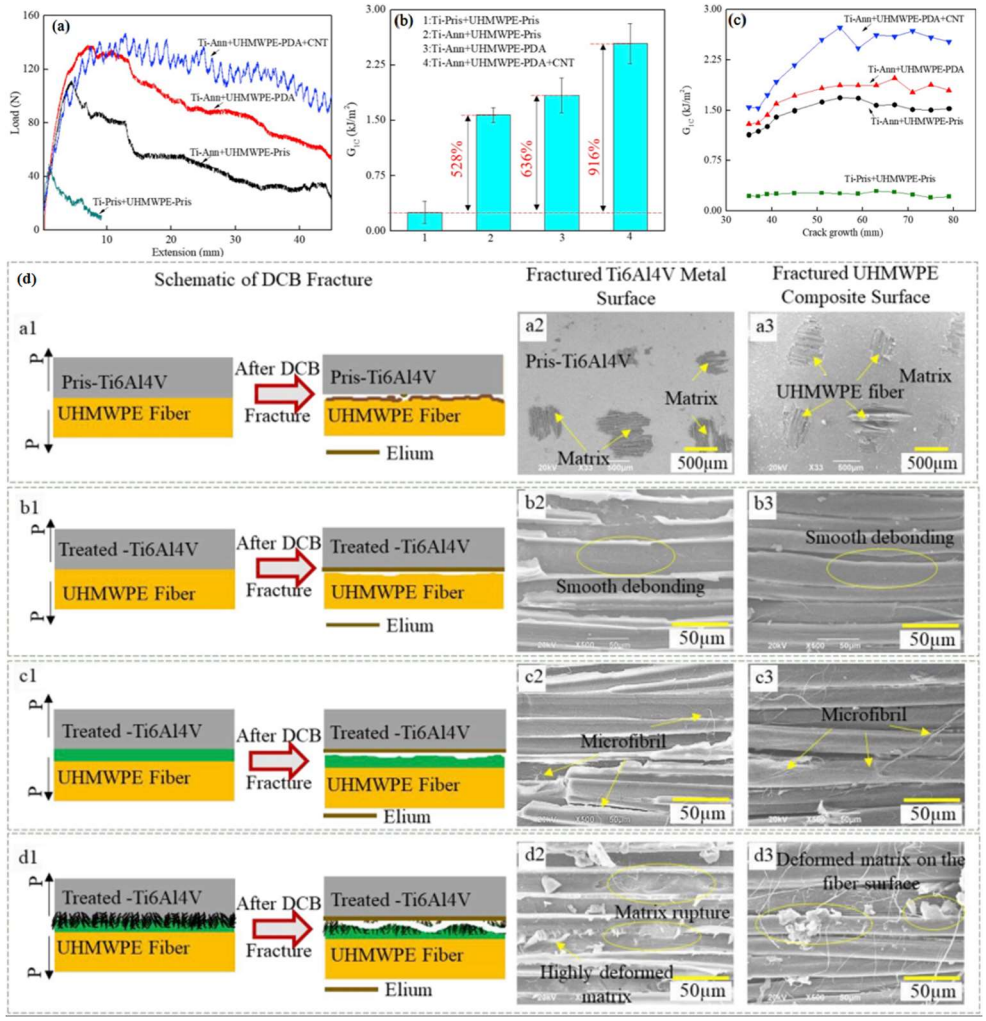

Figure 28. (a) Load-displacement behaviour, (b) Mode-I interlaminar fracture toughness, (c) resistance curves for four FMLs, showing the effects of fibre-surface and metal-surface treatments (Copyright permission from Elsevier. Reproduced from Figs. 5 & 7 in [89]).

7 Important consideration for the use of acrylic resins in composite applications

7.1 History of flammability

Random chain scission was identified as the primary mechanism by which an acrylic polymer undergoes major thermal degradation (Section 2.1.1). This highlights the importance of further exploration of the flammability of reactive acrylic polymers and their composites. Acrylics are known to depolymerise at elevated temperatures owing to the aforementioned scission mechanism, releasing flammable monomers, which pose in-service fire hazard implications. This is particularly important, given the contributions of poly(methyl methacrylate) sheet glazing (Oroglas) to the Summerland disaster in 1973 [90,91]. Already, it has been shown that, by using non-woven intumescent mats [92] and a phosphorus-carbon-based flame retardant [93], that the flame-retardant and smoke suppression properties of acrylic-matrix composites can be significantly enhanced.

7.2 Vulnerability to solvent attack

Furthermore, while the dissolution of acrylic-matrix composites in acetone offers favourable end-of-life resource recovery prospects as discussed in Section 5.3, it highlights the vulnerability of these materials to solvent attack. Low solvent resistance therefore constitutes a challenge to the extended applicability of acrylic-matrix composites.

7.3 Sustainable production and application of bio-based acrylic resins

Finally, considering the ongoing market shift from petroleum-based polymers to bio-based polymers for composite applications, the development and application of reactive bio-based monomers is highly attractive for establishing improved supply chain sustainability [94,95]. In fact, the availability of bio-based variants has been considered a key criterion in the material selection process for composites in marine applications [90]. For the purpose of this review, the term *'bio-based'* is used to imply monomers and polymers produced from bio-sourced feedstock (naturally and bio-engineered). Already, technological advances on the synthesis of bio-acrylate monomers bearing great structural similarity to petroleum-derived acrylates has been demonstrated by Voronov and Tarnavchyk [96,97]. Moreover the use of more

sustainable feedstocks in the production of methyl methacrylates adhesives and monomers by Lucite, Evonik and Arkema holds promise for the exploration of bio-based acrylics [98].

Technological development continues in this area, but thus far, the most viable bio-sources are epoxidised and hydroxylated soybean oil, pine tree resin and various lignin derivatives [95,96,98–101]. While these approaches offer promise for revolutionising the supply chain and environmental impact of thermoplastic acrylic monomers and their end-products, further exploration is critical to continued advancements. Today, bio-based polymers are said to account for less than 1 % of the global production of polymers. Their use is often associated with inferior performance compared to their traditional counterparts [102]. Thus, performance-tailoring research activities aimed at enhancing rigidity, thermal stability and overall compatibility with existing both fibre and sizing technologies, are pivotal to extending their long-term adoption potential. Mono-acrylate isosorbide (derived from cellulose) has been shown to potentially confer favourable thermal and mechanical characteristics on the derived acrylic [103]. The broad availability of bio-feedstocks such as carbohydrates, triglycerides and proteins as viable alternatives to petroleum-based building blocks, therefore offers ecological and technological advantages [104]. Some challenges that need to be overcome in this area for the successful adoption of more sustainable practices includes the lack of cost-competitiveness of bio-renewable feedstocks compared to existing petroleum-based alternatives; an overall lack of maturity; and possibly the true sustainability of feedstocks and synthesis methodologies. The interested reader is referred to an exhaustive overview by Fouilloux and Thomas on current production and polymerisation pathways of bio-based acrylates [102].

7.4 Critical overview of comparative performance

Some characteristics of LRI-processible acrylic polymer (unreinforced) alongside other LRI-processible polymers (isotactic polypropylene and non-aerospace-grade epoxy), and melt-processible isotactic polypropylene can be summarised (as shown in Table 11) to facilitate comparisons between processing routes and attainable properties for different potential applications. In particular, the maximum continuous service temperatures reported in the literature and their resistance to exposure to various conditions and environments are presented to provide an overview of properties, which are expected to directly influence the applicability of these resin systems. Similarly, some representative longitudinal tensile strengths and moduli discussed in this review have been summarised in Figure 29. To provide further insights on the

Table 11. Summary of some comparative attributes of liquid resin infusible acrylic, polyamide-6 and epoxy and melt-processible isotactic polypropylene.

Polymer	*Temperature (°C)*			*Shrinkage*	*Tensile strength*	*Elongation*	*†Avg. material cost*	Water uptake 24 h, 23°C	*Resistance*		
	Processing	*Glass transition*	*Max service*	*(%)*	*(MPa)*	*(%)*	*(£/kg)*	(%)	Solvent	UV	Fuel
Acrylic	25	120	90	0.8	66	3	4.90	0.2-0.4	★	★★★	★★
[LRI]	[27]	[33]	[108]	[109]	[37]	[37]	[110]	[111]	[112]	[112]	[112]
iPP	225	145	130	3	34	350	1.30	0.01-0.1	★	★★	★★
[MP]	[113]	[113]	[108]	[109]	[113]	[113]	[114]	[111]	[112]	[112]	[112]
PA-6	110	65	120	1.6	83	30	1.20	1.6-1.9	★★★★	★★	★★★
[LRI]	[115]	[116]	[108]	[109]	[117]	[117]	[118]	[111]	[112]	[112]	[112]
Epoxy	25	127	90	6.9	78	4	2.40	0.1-0.15	★★★★	★	★★★★
[LRI]‡	[37]	[37]	[119]	[120]	[37]	[37]	[110]	[119]	[121]	[122]	[123]

The numbers in square brackets represent references corresponding to the sourced values; ***iPP****: isotactic polypropylene;* ***PA-6****: polyamide-6;* ***LRI:*** *suited to liquid resin infusing;* ***MP:*** *suited to melt processing;* ‡ *Reported values are from literature/sources on commodity, non-aerospace grade epoxies;* † *£/GBP equivalents as of the 26th of February, 2021 for the €/EUR and $/USD values reported in the referenced sources. The ratings for resistance to exposure under various conditions are: 'Poor (★)', 'Fair (★★)', 'Good (★★★)' and 'Excellent (★★★★)'.*

quality of the interfacial adhesion across these composite systems and variability, theoretical predictions for strengths (Figure 29a) and moduli (Figure 29b) were obtained. This was done for multiaxial carbon, UD glass and woven glass fibre-reinforced acrylics. In the interest of simplicity, multiaxial and woven reinforcements were assumed to offer comparable contributions. Given the similarities between the various grades of the acrylic resin, the predicted properties were relatively consistent across all grades. The interested reader is referred to the supporting document for further methodological information.

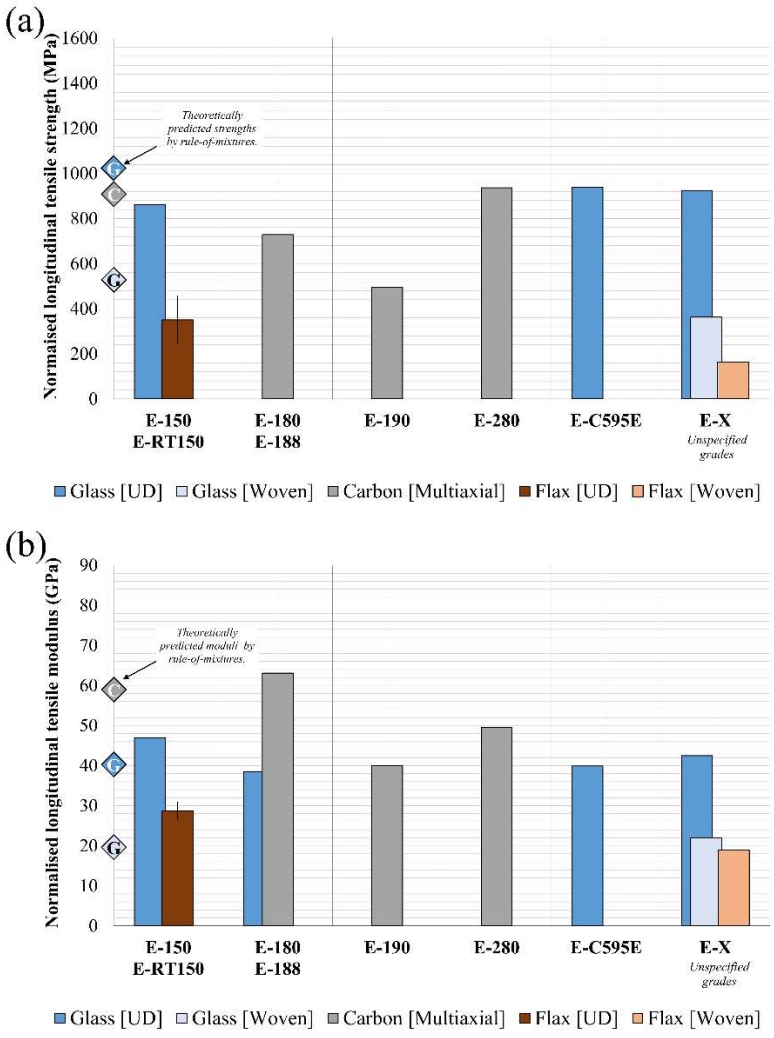

Figure 29. Summary of (a) Vf-normalised longitudinal tensile strengths and (b) corresponding Vf-normalised longitudinal tensile moduli. All reported data were normalised to a Vf of 50% to facilitate comparisons. Respective rule-of-mixtures-derived predictions, labelled C and G (on the y-axis) were assessed for multiaxial carbon, and UD and woven glass materials. The diamond-shaped markers maintain the same colours designation shown in the legend.

As can be seen in Figure 29a, all experimental values were inferior to the theoretical values, with the exception of the multiaxial carbon-reinforced E-280 material, which appeared to be marginally superior. Interestingly, the highly aligned, pultruded UD glass fibre-reinforced E-C595E material exhibits comparable V_f-normalised strength to the multiaxial carbon and UD glass E-150 material. All glass fibre reinforced samples exhibited only marginally lower experiment strength with respect to theoretically-derived strengths. While these results may highlight contributions of the interface and fibre alignment, the theoretical and experimental values appear to be comparable in terms of orders of magnitude. Figure 29b reveals good agreement between experimental and theoretical data.

8 Future research directions

Pivotal to this process is the identification of existing challenges and associated opportunities to steer and guide future research. Already, we have discussed some important consideration and challenges for the adoption of liquid, *in situ* polymerisable acrylic monomer resins into newer application as substitutes for existing polymer and resin technologies. Herein, we present thoughts on gaps in existing contributions and propose further related challenges yet to be addressed.

1. Addressing the current environmental challenges associated with end-of-life decommissioning and waste management will continue to be a key driver of research activities within the composites industry. To futureproof these liquid acrylic resins as ideal candidate materials for a greener market, the following areas are worthy of further exploration:

    a. **Reshapability**: Building on the work of the authors discussed in *Section 5.1*, can large-scale fibre-reinforced acrylics be readily thermoformed to meet the requirements for serial production? Are there viable routes to reuse of reclaimed materials from decommissioned acrylic-based components?
    b. **Recyclability**: In the context of the works reviewed in *Section 5.3*, are there other more environmentally friendly routes to complete reclamation of continuous fibres from acrylic-based composites?

c. **Repairability**: Can the reactivity of liquid acrylic resins be exploited for repair operations? Can large-scale structures be repaired on-site at room temperature without the need for costly decommissioning?

d. **Sustainability**: Can bio-sourced feedstock be reliably and sustainably employed to develop more value-added products based on acrylic monomer technology? Can performance-tailoring be performed to enhance the appeal of bio-derived acrylic building blocks with sustainable natural fibres and other bio-derived monomers, macromonomers and polymers to concomitantly confer desirable functionality?

2. The works discussed in *Section 5.2* on thermally joining acrylic-matrix composites have highlighted the need for scaling joining methodologies for larger structures. The use of conductive heating elements necessitates extensive lightning protection research, particularly for wind turbine blades. The durability of welded joints needs to be investigated, particularly building on the reviewed works on fatigue resistance; investigation of their water absorption behaviour would also be beneficial. Finally, the adaptability of these lab-based joining techniques to field joining operations must be adequately explored.

3. Despite the extensive efforts towards a comprehensive database on the performance of acrylic-matrix composites (*Section 4*), there still exists a paucity of published literature on their compressive performance, long-term durability and resilience, particularly due to the time scales required and the infancy of this resin technology. As such, the exploration of the comparative compressive behaviour, long-term performance (creep and fatigue) and UV sensitivity are essential.

4. While efforts have been made towards enhancing the mechanical and thermomechanical performance of acrylic-matrix composites, the standard practice involves the incorporation of a nanoscale rubber phase into the thermoplastic resin (*Section 4.6*). The use of thermoplastic modifiers remains unexplored for these resins. Furthermore, being amorphous thermoplastics, composites based on these acrylic matrices may exhibit poor solvent resistance as discussed in Section 7. These must also be considered in studies on tailoring of bulk matrix performance. Finally, a complementary approach to assessing the resulting interfaces must be explored.

5. The reactive nature of these liquid resins makes them ideally suited for use in multi-material systems such as fibre-metal laminates, the success of which has been highlighted in *Section* 6 of this review. Extensive exploration of the unique interfaces within such material systems should be undertaken. Moreover, the combination of dissimilar constituents presents unique challenges in terms of thermal expansion coefficient mismatch, moisture sensitivity and non-destructive damage evaluation. These areas may necessitate dedicated research efforts.

6. Innovative process-related research may pave the way for even greater adoption-potential for these reactive thermoplastic acrylic resins. Routes that facilitate the integration of reactive acrylic technology into alternative processing methods; e.g.: prepreg-inspired products with selective activation profiles must be explored. An indicator of innovation in this area is the recent patented approach for preparing acrylic-matrix thermoplastic prepreg composites by Zhang et al. [105]. Extending the technological advancement demonstrated therein requires the exploration of routes to address the challenges posed by the inherent low boiling point of acrylic monomers. The works presented in *Sections 1 & 3* provide an essential foundation on the polymerisation behaviour and current processing methods for these liquid acrylic resin systems. To make these resins successful candidates for industrial applications, the suitable selection of initiators with delayed (or temperature-controlled) activity can be effective for the fabrication of large-scale components in the industrial environment.

9 Concluding remarks

In this paper, the research contributions on *in situ* polymerisable acrylic resins and their composites have been reviewed. From research contributions to-date, their role in the cost-effective production of continuous fibre-reinforced thermoplastics at favourably low temperature and pressures; current challenges, and future research opportunities have also been identified. These matrices have been shown to exhibit competitive thermomechanical and mechanical performance to more established epoxy resin systems. The room temperature infusibility, thermoformability, weldability and recyclability of *in situ* polymerised acrylic-matrix composites have been demonstrated. Based on the trends highlighted in this review of research contributions to-date on *in situ* polymerised acrylic composites, as the demands on industry continue to drive research towards adopting practices for improved circularity, the demand for reactive resin systems

will potentially see high growth. It is our belief that these liquid resins will gain increasing cross-sectoral acceptance, if the challenges in understanding their durability and enhancing their mechanical and thermomechanical performance are addressed.

References

[1] Hinkley J, Johnston N, O'Brien T. Interlaminar fracture toughness of thermoplastic composites. Adv Thermoplast Matrix Compos Mater 1989:251–63. https://doi.org/10.1520/stp24606s.

[2] Nash NH, Young TM, McGrail PT, Stanley WF. Inclusion of a thermoplastic phase to improve impact and post-impact performances of carbon fibre reinforced thermosetting composites - A review. Mater Des 2015;85:582–97. https://doi.org/10.1016/j.matdes.2015.07.001.

[3] Kim K-Y, Ye L, Phoa K-M. Interlaminar fracture toughness of CF/PEI and GF/PEI composites at elevated temperatures. Appl Compos Mater 2004;11:173–90.

[4] Howes JC, Loos AC, Hinkley JA. The effect of processing on autohesive strength development in thermoplastic resins and composites. In: Newaz GM, editor. Adv. Thermoplast. Matrix Compos. Mater. ASTM STP 1044, Florida: American Society for Testing and Materials; 2008, p. 33–49. https://doi.org/10.1520/stp24593s.

[5] Akca E, Gursel A. A Review on the Matrix Toughness of Thermoplastic Materials. Period Eng Nat Sci 2015;3:1–8. https://doi.org/10.21533/pen.v3i2.52.

[6] Coll SM, Murtagh AM, Ó Brádaigh CM. Resin film infusion of cyclic pBT composites: a fundamental study. Proc. SAMPE Eur. 25th Int. Jubil. Conf., Paris: 2004.

[7] Parton H, Verpoest I. In situ polymerization of thermoplastic composites based on cyclic oligomers. Polym Compos 2005;26:60–5.

[8] Yan C, Liu L, Zhu Y, Xu H, Liu D. Properties of polymerized cyclic butylene terephthalate and its composites via ring-opening polymerization. J Thermoplast Compos Mater 2018;31:181–201. https://doi.org/10.1177/0892705717697774.

[9] Abt T, Sánchez-Soto M. A review of the recent advances in cyclic butylene terephthalate technology and its composites. Crit Rev Solid State Mater Sci 2017;42:173–217. https://doi.org/10.1080/10408436.2016.1160820.

[10] Balogh G. Development of cyclic butylene terephthalate matrix composites. Budapest University of Technology and Economics [Doctoral Thesis], 2012.

[11] Van Rijswijk K, Teuwen JJE, Bersee HEN, Beukers A. Textile fiber-reinforced anionic polyamide-6 composites. Part I: The vacuum infusion process. Compos Part A Appl Sci Manuf 2008;40:1–10. https://doi.org/10.1016/j.compositesa.2008.03.018.

[12] Pillay S, Vaidya UK, Janowski GM. Effects of moisture and UV exposure on liquid molded carbon fabric reinforced nylon 6 composite laminates. Compos Sci Technol 2009;69:839–46. https://doi.org/10.1016/j.compscitech.2008.03.021.

[13] Ó Máirtín P, McDonnell P, Connor M, Eder R, Ó Brádaigh CM. Process investigation of a liquid PA-12/carbon fibre moulding system. Compos Part A 2001;32:915–23.

[14] Zingraff L, Michaud V, Bourban PE, Månson JAE. Resin transfer moulding of anionically polymerised polyamide 12. Compos Part A Appl Sci Manuf 2005;36:1675–86. https://doi.org/10.1016/j.compositesa.2005.03.023.

[15] Ó Brádaigh CM, Doyle A, Doyle D, Feerick P. Electrically-heated ceramic composite tooling for out-of-autoclave manufacturing of large composite structures. SAMPE J 2011;47:6–14.

[16] Doyle A, Feerick P, Mallon P, Ó Brádaigh C, Doyle D. A heated mould for moulding polymeric composites, a method for making such mould and its use. European Patent EP 2344312B1, 2012.

[17] Gardiner G. Thermoplastic wind blades: To be or Not? CompositesWorld 2012:30–5. http://www.compositesworld.com/articles/thermoplastic-wind-blades-to-be-or-not.

[18] van Rijswijk K, Bersee HEN. Reactive processing of textile fiber-reinforced thermoplastic composites - An overview. Compos Part A Appl Sci Manuf 2007;38:666–81. https://doi.org/10.1016/j.compositesa.2006.05.007.

[19] Murray RE, Snowberg D, Berry D, Beach R, Rooney S, Swan D. Manufacturing a 9-meter thermoplastic composite wind turbine blade. Am. Soc. Compos. 32nd Tech. Conf., West Lafayette, Indiana: 2017.

[20] Arkema. Elium resin: a disruptive innovation in the world of composites. Innov Webzine 2019. https://www.arkema.com/global/en/webzine/post/elium-resin-a-disruptive-innovation-in-the-world-of-composites/.

[21] Murray RE, Beach R, Barnes D, Snowberg D, Berry D, Rooney S, et al. Structural validation of a thermoplastic composite wind turbine blade with comparison to a thermoset composite blade. Renew Energy 2021;164:1100–7. https://doi.org/10.1016/j.renene.2020.10.040.

[22] Cousins DS, Suzuki Y, Murray RE, Samaniuk JR, Stebner AP. Recycling glass fiber thermoplastic composites from wind turbine blades. J Clean Prod 2019;209:1252–63. https://doi.org/10.1016/j.jclepro.2018.10.286.

[23] Ehrenstein GW. Polymeric materials. Munich: Carl Hanser Verlag; 2001.

[24] McCrum NG, Buckley CP, Bucknall CB. Principles of polymer engineering. 2nd ed. Oxford University Press; 1997.

[25] de Andrade Raponi O, Barbosa LCM, de Souza BR, Ancelotti Junior AC. Study of the influence of initiator content in the polymerization reaction of a thermoplastic liquid resin for advanced composite manufacturing. Adv Polym Technol 2018;37:3579–87. https://doi.org/10.1002/adv.22142.

[26] de Andrade Raponi O, de Souza BR, Barbosa LCM, Ancelotti Junior AC. Thermal, rheological, and dielectric analyses of the polymerization reaction of a liquid thermoplastic resin for infusion manufacturing of composite materials. Polym Test 2018;71:32–7. https://doi.org/10.1016/j.polymertesting.2018.08.024.

[27] Arkema. ELIUM® 150 technical datasheet – Liquid thermoplastic resin for glass-reinforced composite 2017. https://cstjmateriauxcomposites.files.wordpress.com/2017/11/elium_150_tech_data_sheet_grp_160908.pdf (accessed December 21, 2020).

[28] Murray RE, Penumadu D, Cousins D, Beach R, Snowberg D, Berry D, et al. Manufacturing and Flexural Characterization of Infusion-Reacted Thermoplastic Wind Turbine Blade Subcomponents. Appl Compos Mater 2019;27:1–17. https://doi.org/10.1007/s10443-019-9760-2.

[29] Charlier Q, Fontanier J-C, Lortie F, Pascault J-P, Gerard J-F. Rheokinetic study of acrylic reactive mixtures dedicated to fast processing of fiber-reinforced thermoplastic composites. J Appl Polym Sci 2019;136:47391. https://doi.org/10.1002/app.47391.

[30] Pantelelis N, Bistekos E, Emmerich R, Gerard P, Zoller A, Gallardo RR. Compression RTM of reactive thermoplastic composites using microwaves and cure monitoring. Procedia CIRP 2019;85:249–54. https://doi.org/10.1016/j.procir.2019.10.005.

[31] Han N, Baran I, Zanjani JSM, Yuksel O, An LL, Akkerman R. Experimental and computational analysis of the polymerization overheating in thick glass/Elium® acrylic thermoplastic resin composites. Compos Part B Eng 2020. https://doi.org/10.1016/j.compositesb.2020.108430.

[32] Matadi Boumbimba R, Coulibaly M, Khabouchi A, Kinvi-Dossou G, Bonfoh N, Gerard P. Glass fibres reinforced acrylic thermoplastic resin-based tri-block copolymers composites: Low velocity impact response at various temperatures. Compos Struct 2017;160:939–51. https://doi.org/10.1016/j.compstruct.2016.10.127.

[33] Bhudolia SKK, Perrotey P, Joshi SCC. Optimizing polymer infusion process for thin ply textile composites with novel matrix system. Materials (Basel) 2017;10. https://doi.org/10.3390/ma10030293.

[34] Bhudolia SK, Joshi SC. Low-velocity impact response of carbon fibre composites with novel liquid Methylmethacrylate thermoplastic matrix. Compos Struct 2018;203:696–708. https://doi.org/10.1016/j.compstruct.2018.07.066.

[35] Bhudolia SK, Perrotey P, Joshi SC. Experimental investigation on suitability of carbon fibre thin plies for racquets. Proc Inst Mech Eng Part P J Sport Eng Technol 2016;230:64–72. https://doi.org/10.1177/1754337115598489.

[36] Lorriot T, El Yagoubi J, Fourel J, Tison F. Non-conventional glass fiber NCF composites with thermoset and thermoplastic matrices. 20th Int. Conf. Compos. Mater., Copenhagen: 2015.

[37] Obande W, Mamalis D, Ray D, Yang L, Ó Brádaigh CM. Mechanical and thermomechanical characterisation of vacuum-infused thermoplastic- and thermoset-based composites. Mater Des 2019;175:107828. https://doi.org/10.1016/j.matdes.2019.107828.

[38] Murray RE, Roadman J, Beach R. Fusion joining of thermoplastic composite wind turbine blades: Lap-shear bond characterization. Renew Energy 2019;140:501–12. https://doi.org/10.1016/j.renene.2019.03.085.

[39] Bhudolia SK, Gohel G, Kah Fai L, Barsotti RJ. Fatigue response of ultrasonically welded carbon/Elium® thermoplastic composites. Mater Lett 2020;264:127362. https://doi.org/10.1016/j.matlet.2020.127362.

[40] Boufaida Z, Farge L, André S, Meshaka Y. Influence of the fiber/matrix strength on the mechanical properties of a glass fiber/thermoplastic-matrix plain weave fabric composite. Compos Part A Appl Sci Manuf 2015;75:28–38. https://doi.org/10.1016/j.compositesa.2015.04.012.

[41] Baley C, Lan M, Bourmaud A, Le Duigou A. Compressive and tensile behaviour of unidirectional composites reinforced by natural fibres: Influence of fibres (flax and jute), matrix and fibre volume fraction. Mater Today Commun 2018;16:300–6. https://doi.org/10.1016/j.mtcomm.2018.07.003.

[42] Hindersmann A. Confusion about infusion: An overview of infusion processes. Compos Part A Appl Sci Manuf 2019. https://doi.org/10.1016/j.compositesa.2019.105583.

[43] Afendi M, Banks WM, Kirkwood D. Bubble free resin for infusion process. Compos Part A Appl Sci Manuf 2005;36:739–46. https://doi.org/10.1016/j.compositesa.2004.10.030.

[44] Obande W, Ó Brádaigh CM, Ray D. Thermoplastic hybrid-matrix composite prepared by a room-temperature vacuum infusion and *in situ* polymerisation process. Compos Commun 2020. https://doi.org/10.1016/j.coco.2020.100439.

[45] Chilali A, Zouari W, Assarar M, Kebir H, Ayad R. Analysis of the mechanical behaviour of flax and glass fabrics-reinforced thermoplastic and thermoset resins. J Reinf Plast Compos 2016;35:1217–32. https://doi.org/10.1177/0731684416645203.

[46] Cousins DS. Advanced thermoplastic composites for wind turbine blade manufacturing. Colorado School of Mines [Doctoral Thesis], 2018.

[47] Zoller A, Escalé P, Gérard P. Pultrusion of bendable continuous fibers reinforced composites with reactive acrylic thermoplastic Elium® resin. Front Mater 2019;6:1–9. https://doi.org/10.3389/fmats.2019.00290.

[48] Lee J, Soutis C. A study on the compressive strength of thick carbon fibre-epoxy laminates. Compos Sci Technol 2007;67:2015–26. https://doi.org/10.1016/j.compscitech.2006.12.001.

[49] Davies P, Arhant M. Fatigue behaviour of acrylic matrix composites: influence of seawater. Appl Compos Mater 2019;26:507–18. https://doi.org/10.1007/s10443-018-9713-1.

[50] Arkema. Liquid thermoplastic resin for tougher composites n.d.;1. https://www.arkema-americas.com/export/shared/.content/media/downloads/products-documentations/incubator/brochure-elium-2017.pdf.

[51] Obande W, Ray D, Ó Brádaigh CM. Viscoelastic and drop-weight impact properties of an acrylic-matrix composite and a conventional thermoset composite – A comparative study. Mater Lett 2019;238:38–41. https://doi.org/10.1016/j.matlet.2018.11.137.

[52] Kinvi-Dossou G, Matadi Boumbimba R, Bonfoh N, Garzon-Hernandez S, Garcia-Gonzalez D, Gerard P, et al. Innovative acrylic thermoplastic composites versus conventional composites: Improving the impact performances. Compos Struct 2019;217:1–13.

https://doi.org/10.1016/j.compstruct.2019.02.090.

[53] Pini T. Fracture behaviour of thermoplastic acrylic resins and their relevant unidirectional carbon fibre composites: rate and temperature effects. Politecnico Milano 1863 [Doctoral Thesis], 2017.

[54] Cadieu L, Kopp JB, Jumel J, Bega J, Froustey C. Strain rate effect on the mechanical properties of a glass fibre reinforced acrylic matrix laminate. An experimental approach. Compos Struct 2019;223:110952. https://doi.org/10.1016/j.compstruct.2019.110952.

[55] Bhudolia SK, Joshi SC, Bert A, Di YB, Makam R, Gohel G. Flexural characteristics of novel carbon methylmethacrylate composites. Compos Commun 2019;13:129–33. https://doi.org/10.1016/j.coco.2019.04.007.

[56] Bhudolia SK, Joshi SC, Bert A, Gohel GR, Raama M. Energy Characteristics and Failure Mechanisms for Textile Spread Tow Thin Ply Thermoplastic Composites under Low-velocity Impact. Fibers Polym 2019;20:1716–25. https://doi.org/10.1007/s12221-019-9295-z.

[57] Bhudolia SK, Perrotey P, Joshi SC. Mode I fracture toughness and fractographic investigation of carbon fibre composites with liquid Methylmethacrylate thermoplastic matrix. Compos Part B Eng 2018;134:246–53. https://doi.org/10.1016/j.compositesb.2017.09.057.

[58] Barbosa LCM, Bortoluzzi DB, Ancelotti AC. Analysis of fracture toughness in mode II and fractographic study of composites based on Elium® 150 thermoplastic matrix. Compos Part B Eng 2019;175:107082. https://doi.org/10.1016/j.compositesb.2019.107082.

[59] Haggui M, El Mahi A, Jendli Z, Akrout A, Haddar M. Damage analysis of flax fibre/elium composite under static and fatigue testing. In: Haddar M, Chaari F, Benamara A, Chouchane M, Karra C, Aifaoui N, editors. Des. Model. Mech. Syst., Cham: Springer International Publishing; 2018, p. 681–91.

[60] Haggui M, El Mahi A, Jendli Z, Akrout A, Haddar M. Static and fatigue characterization of flax fiber reinforced thermoplastic composites by acoustic emission. Appl Acoust 2019;147:100–10. https://doi.org/10.1016/j.apacoust.2018.03.011.

[61] Virk AS, Hall W, Summerscales J. Failure strain as the key design criterion for fracture of natural fibre composites. Compos Sci Technol 2010;70:995–9. https://doi.org/10.1016/j.compscitech.2010.02.018.

[62] Barbosa LCM, Gomes G, Junior ACA. Prediction of temperature-frequency-dependent mechanical properties of composites based on thermoplastic liquid resin reinforced with carbon fibers using artificial neural networks. Int J Adv Manuf Technol 2019. https://doi.org/10.1007/s00170-019-04486-4.

[63] Bhudolia SK, Perrotey P, Joshi SC. Enhanced vibration damping and dynamic mechanical characteristics of composites with novel pseudo-thermoset matrix system. Compos Struct 2017;179:502–13. https://doi.org/10.1016/j.compstruct.2017.07.093.

[64] Pini T, Caimmi F, Briatico-Vangosa F, Frassine R, Rink M. Fracture initiation and propagation in unidirectional CF composites based on thermoplastic acrylic resins. Eng Fract Mech 2017;184:51–

8. https://doi.org/10.1016/j.engfracmech.2017.08.023.

[65] Pini T, Briatico-Vangosa F, Frassine R, Rink M. Time dependent fracture behaviour of a carbon fibre composite based on a (rubber toughened) acrylic polymer. Procedia Struct Integr 2016;2:253–60. https://doi.org/10.1016/j.prostr.2016.06.033.

[66] Johanna B, Jean-François G, Frédéric L, Pierre G, Jérôme M. New continuous fiber reinforced thermoplastic composites: An analysis of interfacial adhesion from the micro scale to the macro scale. ICCM Int Conf Compos Mater 2015;2015-July:19–24.

[67] Davies P, Le Gac PYY, Le Gall M. Influence of sea water aging on the mechanical behaviour of acrylic matrix composites. Appl Compos Mater 2017;24:97–111. https://doi.org/10.1007/s10443-016-9516-1.

[68] Shanmugam L, Kazemi ME, Rao Z, Lu D, Wang X, Wang B, et al. Enhanced Mode I fracture toughness of UHMWPE fabric/thermoplastic laminates with combined surface treatments of polydopamine and functionalized carbon nanotubes. Compos Part B Eng 2019;178:107450. https://doi.org/10.1016/j.compositesb.2019.107450.

[69] Charlier Q, Lortie F, Gerard P, Gerard JF. Interfacial adhesion between glass fibers and acrylic-based matrices as studied by micromechanical testing. ICCM Int Conf Compos Mater 2015;2015-July:19–24.

[70] Thomason JL. Glass fibre sizing: A review. Compos Part A Appl Sci Manuf 2019;127. https://doi.org/10.1016/j.compositesa.2019.105619.

[71] Pini T, Briatico-Vangosa F, Frassine R, Rink M. Matrix toughness transfer and fibre bridging laws in acrylic resin based CF composites. Eng Fract Mech 2018;203:115–25. https://doi.org/10.1016/j.engfracmech.2018.03.026.

[72] Pini T, Castellani L, Briatico-Vangosa F, Frassine R, Rink M. Damage mechanisms in a toughened acrylic resin: Effect of temperature and thermal history. Polym Eng Sci 2019;59:566–72. https://doi.org/10.1002/pen.24971.

[73] Pini T, Briatico-Vangosa F, Frassine R, Rink M. Fracture toughness of acrylic resins: Viscoelastic effects and deformation mechanisms. Polym Eng Sci 2018;58:369–76. https://doi.org/10.1002/pen.24583.

[74] Keskin R, Adanur S. Improving toughness of polypropylene with thermoplastic elastomers in injection molding. Polym - Plast Technol Eng 2011;50:20–8. https://doi.org/10.1080/03602559.2010.512344.

[75] Tamas-Benyei P, Bitay E, Kishi H, Matsuda S, Czigany T. Toughening of epoxy resin: The effect of water jet milling on worn tire rubber particles. Polymers (Basel) 2019;11. https://doi.org/10.3390/polym11030529.

[76] Utaloff K, Kothmann MH, Ciesielski M, Döring M, Neumeyer T, Altstädt V, et al. Improvement of fracture toughness and glass transition temperature of DGEBA-based epoxy systems using toughening and crosslinking modifiers. Polym Eng Sci 2019;59:86–95.

https://doi.org/10.1002/pen.24870.

[77] Barsotti R, Fine T, Inoubli R, Gerard P, Schmidt S, Macy N, et al. Nanostrength ® Block Copolymers for Epoxy Toughening 2008. https://www.trfa.org/erc/docretrieval/uploadedfiles/Technical Papers/2008 Meeting/Barsotti-Arkema_paper-Block_copolymers.pdf.

[78] Bhudolia SK, Gohel G, Fai LK, Barsotti RJ. Investigation on ultrasonic welding attributes of novel carbon/Elium® composites. Materials (Basel) 2020;13:10–5. https://doi.org/10.3390/ma13051117.

[79] Gebhardt M, Chakraborty S, Manolakis I, Meiners D. Closed-loop room temperature recycling of Elium CFRPs and its influence on the 2nd generation composite properties. J Sci Alliance Plast Technol 2020;16:179–210.

[80] Lee P, Sims E, Bertham O, Symington H, Bell N, Pfaltzgraff L, et al. Towards a circular economy – waste management in the EU 2017. https://www.europarl.europa.eu/RegData/etudes/STUD/2017/581913/EPRS_STU%282017%29581913_EN.pdf (accessed February 24, 2021).

[81] Summerscales J, Singh MM, Wittamore K. Disposal of composite boats and other marine composites. Mar. Appl. Adv. Fibre-Reinforced Compos., Elsevier Inc.; 2016, p. 185–213. https://doi.org/10.1016/B978-1-78242-250-1.00008-9.

[82] Safri SNA, Sultan MTH, Jawaid M, Jayakrishna K. Impact behaviour of hybrid composites for structural applications: A review. Compos Part B Eng 2018;133:112–21. https://doi.org/10.1016/j.compositesb.2017.09.008.

[83] Bunea M, Cîrciumaru A, Buciumeanu M, Bîrsan IG, Silva FS. Low velocity impact response of fabric reinforced hybrid composites with stratified filled epoxy matrix 2018. https://doi.org/10.1016/j.compscitech.2018.11.024.

[84] Kazemi MEE, Shanmugam L, Lu D, Wang X, Wang B, Yang J. Mechanical properties and failure modes of hybrid fiber reinforced polymer composites with a novel liquid thermoplastic resin, Elium®. Compos Part A Appl Sci Manuf 2019;125:105523. https://doi.org/10.1016/j.compositesa.2019.105523.

[85] Kazemi ME, Shanmugam L, Dadashi A, Shakouri M, Lu D, Du Z, et al. Investigating the roles of fiber, resin, and stacking sequence on the low-velocity impact response of novel hybrid thermoplastic composites. Compos Part B Eng 2021;207:108554. https://doi.org/10.1016/j.compositesb.2020.108554.

[86] Vlot A, Gunnik JW. Fibre metal laminates: an introduction. 2011. https://doi.org/DOI 10.1007/978-94-010-0995-9.

[87] Vogelesang LB, Vlot A. Development of fibre metal laminates for advanced aerospace structures. J Mater Process Technol 2000;103:1–5. https://doi.org/10.1016/S0924-0136(00)00411-8.

[88] Mamalis D, Obande W, Koutsos V, Blackford JR, Ó Brádaigh CM, Ray D. Novel thermoplastic fibre-metal laminates manufactured by vacuum resin infusion: The effect of surface treatments on

interfacial bonding. Mater Des 2019;162:331–44. https://doi.org/10.1016/j.matdes.2018.11.048.

[89] Shanmugam L, Kazemi ME, Rao Z, Yang L, Yang J. On the metal thermoplastic composite interface of Ti alloy/UHMWPE-Elium® laminates. Compos Part B Eng 2020;181:107578. https://doi.org/10.1016/j.compositesb.2019.107578.

[90] Qin Y, Summerscales J, Graham-Jones J, Meng M, Pemberton R. Monomer selection for in situ polymerization infusion manufacture of natural-fiber reinforced thermoplastic-matrix marine composites. Polymers (Basel) 2020;12:1–25. https://doi.org/10.3390/polym12122928.

[91] National Materials Advisory Board, Sciences NA of. Fire Safety Aspects of Polymeric Materials, Volume 1. National Academy of Sciences; 1977.

[92] Khalili P, Blinzler B, Kádár R, Blomqvist P, Sandinge A, Bisschop R, et al. Ramie fabric Elium® composites with flame retardant coating: Flammability, smoke, viscoelastic and mechanical properties. Compos Part A Appl Sci Manuf 2020;137:105986. https://doi.org/10.1016/j.compositesa.2020.105986.

[93] Khalili P, Blinzler B, Kádár R, Bisschop R, Försth M, Blomqvist P. Flammability, smoke, mechanical behaviours and morphology of flame retarded natural fibre/Elium® composite. Materials (Basel) 2019;12. https://doi.org/10.3390/ma12172648.

[94] Sun XS. Overview of Plant Polymers: Resources, Demands, and Sustainability. Bio-Based Polym. Compos., 2005, p. 1–14. https://doi.org/https://doi.org/10.1016/B978-0-12-763952-9.X5000-X.

[95] Wu N, Demchuk Z, Voronov A, Pourhashem G. Sustainable manufacturing of polymeric materials: A techno-economic analysis of soybean oil-based acrylic monomers production. J Clean Prod 2021;286. https://doi.org/10.1016/j.jclepro.2020.124939.

[96] Voronov A, Tarnavchyk I. Bio-based acrylic monomers. United States Patent US10315985B2, 2019.

[97] Voronov A, Tarnavchyk I. Bio-based acrylic monomers and polymers thereof. United States Patent US10584094B2, 2020.

[98] Sweeney N. Biobased acrylic adhesives. Handb. Adhes. Technol. Third Ed., 2017. https://doi.org/10.1201/9781315120942.

[99] Tajbakhsh S, Hajiali F, Maric M. Nitroxide-mediated miniemulsion polymerization of bio-based methacrylates. Ind Eng Chem Res 2020. https://doi.org/10.1021/acs.iecr.0c00840.

[100] Lebeau J, Efromson JP, Lynch MD. A Review of the Biotechnological Production of Methacrylic Acid. Front Bioeng Biotechnol 2020. https://doi.org/10.3389/fbioe.2020.00207.

[101] Veith C, Diot-Néant F, Miller SA, Allais F. Synthesis and polymerization of bio-based acrylates: A review. Polym Chem 2020;11:7452–70. https://doi.org/10.1039/d0py01222j.

[102] Fouilloux H, Thomas CM. Production and polymerization of biobased acrylates and analogs. Macromol Rapid Commun 2021;42. https://doi.org/10.1002/marc.202000530.

[103] Veregin RPN, Sacripante GG. Bio-based acrylate and (meth)acrylate resins. United States Patent US9581924B2, 2014.

[104] Yu D, Zhao J, Wang W, Qi J, Hu Y. Mono-acrylated isosorbide as a bio-based monomer for the improvement of thermal and mechanical properties of poly(methyl methacrylate). RSC Adv 2019;9:35532–8. https://doi.org/10.1039/c9ra07548h.

[105] Zhang M, Gleich KF, Yohannes A, Block MJ, Asrar J, Bristol DC, et al. System for producing a fully impregnated thermoplastic prepreg. United States Patent US20200368979A1, 2020.

[106] Fredi G, Dorigato A, Pegoretti A. Novel reactive thermoplastic resin as a matrix for laminates containing phase change microcapsules. Polym Compos 2019. https://doi.org/10.1002/pc.25233.

[107] Monti A, El Mahi A, Jendli Z, Guillaumat L. Mechanical behaviour and damage mechanisms analysis of a flax-fibre reinforced composite by acoustic emission. Compos Part A Appl Sci Manuf 2016;90:100–10. https://doi.org/10.1016/j.compositesa.2016.07.002.

[108] SpecialChem SA. Maximum Continuous Service Temperature. Max Contin Serv Temp 2021. https://omnexus.specialchem.com/polymer-properties/properties/max-continuous-service-temperature (accessed February 23, 2021).

[109] SpecialChem SA. Shrinkage Value of Plastics Material. Shrinkage Value Plast Mater 2021. https://omnexus.specialchem.com/polymer-properties/properties/shrinkage (accessed February 23, 2021).

[110] Murray RE, Jenne S, Snowberg D, Berry D, Cousins D. Techno-economic analysis of a megawatt-scale thermoplastic resin wind turbine blade. Renew Energy 2019;131:111–9. https://doi.org/10.1016/j.renene.2018.07.032.

[111] SpecialChem SA. Water Absorption 24 Hour - (ASTM D570) Test of Plastics n.d. https://omnexus.specialchem.com/polymer-properties/properties/water-absorption-24-hours (accessed February 23, 2021).

[112] RTP Co. Chemical & Environmental Resistance of Thermoplastics. Chem Environ Resist Thermoplast 2021. https://www.rtpcompany.com/technical-info/chemical-resistance/ (accessed February 23, 2021).

[113] Maddah HA. Polypropylene as a Promising Plastic: A Review. Am J Polym Sci 2016;6:1–11. https://doi.org/10.5923/j.ajps.20160601.01.

[114] Plastic Portal. Average Resin Prices I PlasticPortal.eu n.d. https://www.plasticportal.eu/en/polymer-prices/lm/14/ (accessed February 23, 2021).

[115] van Rijswijk K, van Geenen AA, Bersee HEN. Textile fiber-reinforced anionic polyamide-6 composites. Part II: Investigation on interfacial bond formation by short beam shear test. Compos Part A Appl Sci Manuf 2009. https://doi.org/10.1016/j.compositesa.2009.02.018.

[116] van Rijswijk K, Lindstedt S, Vlasveld DPN, Bersee HEN, Beukers A. Reactive processing of anionic polyamide-6 for application in fiber composites: A comparitive study with melt processed polyamides and nanocomposites. Polym Test 2006. https://doi.org/10.1016/j.polymertesting.2006.05.006.

[117] Murray JJ, Robert C, Gleich K, McCarthy ED, Ó Brádaigh CM. Manufacturing of unidirectional

stitched glass fabric reinforced polyamide 6 by thermoplastic resin transfer moulding. Mater Des 2020;189. https://doi.org/10.1016/j.matdes.2020.108512.

[118] SunSirs. SunSirs: Caprolactam Price Was from Rising to Falling in June, How Is the Market Going in the Future? SunSirs Caprolactam Price Was from Rising to Falling June, How Is Mark Going Futur 2020. http://www.sunsirs.com/uk/detail_news-2845.html (accessed February 23, 2021).

[119] East Coast Fibreglass Supplies. EC157 Epoxy Infusion Resin Technical Data Sheet. Tech Data Sheet n.d. http://www.ecfibreglasssupplies.co.uk/images/TechnicalDataSheet/3207.pdf (accessed February 23, 2021).

[120] Li C, Potter K, Wisnom MR, Stringer G. *In situ* measurement of chemical shrinkage of MY750 epoxy resin by a novel gravimetric method. Compos Sci Technol 2004;64:55–64. https://doi.org/10.1016/S0266-3538(03)00199-4.

[121] Zheng S, Lucas PA. Understanding Chemical Resistance In Epoxy System. Underst Chem Resist Epoxy Syst 2020. https://www.coatingsworld.com/issues/2020-06-01/view_technical-papers/understanding-chemical-resistance-in-epoxy-system/ (accessed February 23, 2021).

[122] Nikafshar S, Zabihi O, Ahmadi M, Mirmohseni A, Taseidifar M, Naebe M. The effects of UV light on the chemical and mechanical properties of a transparent epoxy-diamine system in the presence of an organic UV absorber. Materials (Basel) 2017. https://doi.org/10.3390/ma10020180.

[123] Engineering ToolBox. Epoxy - Chemical Resistance. Epoxy - Chem Resist 2004. https://www.engineeringtoolbox.com/chemical-resistance-epoxy-d_786.html (accessed February 23, 2021).